1978AJ.....83..704B

THE ASTRONOMICAL JOURNAL VOLUME 83, NUMBER 7 JULY 1978

EXTENDED RADIO SOURCES AND ELLIPTICAL GALAXIES. I. SMALL-DIAMETER COMPONENTS IN EXTENDED STRUCTURES

A. H. BRIDLE
Queen's University at Kingston, Ontario, Canada K7L 3N6

E. B. FOMALONT
National Radio Astronomy Observatory, Green Bank, West Virginia 24944

Received 15 February 1978

ABSTRACT

High-resolution observations at 2.7 and 8.1 GHz are presented for 48 extended radio galaxies at $\delta > +15°$ containing small-diameter (generally <3 arcsec) components. For most sources baselines up to 35.3 km have been used, providing angular resolutions of a few tenths of an arc second. Accurate positions, flux densities, and angular sizes are given for the small-diameter components and synthesis maps of the extended structures of 23 sources are shown. This paper deals primarily with small "core" components within elliptical galaxies, as opposed to "hot spots" in radio lobes. The source sample preferentially includes optically bright galaxies and hence favors radio sources with luminosities below that at which "hot spots" in radio lobes become prominent; consequently, only three of the small-diameter components reported here prove to be at "end-of-lobe" locations in basically double structures. Two distinguishable types of small component are found at the centers of elliptical galaxies with extended radio emission—compact cores with 2.7–8.1 GHz spectral indices <0.4 and linear sizes typically $\ll 1$ kpc, and extended cores with spectral indices >0.4 and linear sizes typically several kpc. The extended cores exhibit significant correlation between 2.7–8.1 GHz spectral index and 2.7-GHz luminosity; the compact cores do not, possibly due to self-absorption. No significant correlations are found between core parameters and those of the overall radio source, although selection effects produce the appearance of correlation between compact core luminosity and overall luminosity. Our optical identifications based on detection of radio cores in the centers of galaxies validate the traditional use of radio centroids as guides to identifying double sources; furthermore, the radio cores have usually been found in the brightest identification candidate within the extended double structure.

I. INTRODUCTION

This paper is the first of a series reporting new high-resolution observations of several hundred radio galaxies with the NRAO interferometer at 2.7 and 8.1 GHz and with the VLA at 4.9 GHz. The ultimate aim of these observations is to study the relationship between the gross features of extended radio galaxies and (a) their orientation relative to their parent optical objects and (b) the current activity of the galaxies as evidenced by radio emission within their optical boundaries. In this paper we present results on 48 extended radio galaxies at $\delta > +15°$ in which we have detected small-diameter (<3 arcsec) components. Forty-four of these components are located at the centers of elliptical or S0 galaxies and establish the optical identification of the extended emission beyond reasonable doubt. Their detailed structures and orientations will be important parameters for tests of models for the energy reservoirs and collimation processes in radio galaxies.

Section II gives a general description of the source sample which forms the basis of this series of papers and outlines our observing and data reduction procedures. Section III presents radio data on the small-diameter components and on the extended emission containing them. Section IV describes the resulting optical identifications and Sec. V analyzes the physical properties of the small components. Section VI discusses the implications of this work for identifications of extended sources which do not have detectable small-diameter components. The main conclusions of the paper are summarized in Sec. VII.

II. THE OBSERVATIONS

a) The Source Sample

In 1973 G. W. Brandie and the authors culled the astronomical literature to obtain a list of known radio sources purportedly identified with elliptical or S0 galaxies. The quality of radio identifications in the literature at this time varied considerably, so the resulting list of ~1100 "radio galaxies" was far from uniformly reliable. The blue- and red-sensitive *National Geographic Society—Palomar Observatory Sky Atlas* prints were therefore inspected at what we judged to be the best published radio position for each source. Our primary

 0004-6256/78/8307-0704$00.90 © 1978 Am. Astron. Soc.

© American Astronomical Society • Provided by the NASA Astrophysics Data System

1978AJ.....83..704B

TABLE I. Parameters of the NRAO 4-element interferometer.

Operating Frequency (GHz)	2.695	8.085
Bandwidth[a] (MHz)	30	30
System Temperature (K)	105	120
Three 85-ft (26-m) antennas:	Shortest Baseline . . . 100 m	
(Green Bank, W. Va.)	Longest Baseline . . . 2700 m	
One 45-ft (14-m) antenna:	Longest Baseline . . . 35.3 km	
(Huntersville, W. Va.)	to Green Bank	

[a] In each of two circular polarizations, which were averaged together for the present work

aim at this time was to find radio galaxies whose optical elongations would be measurable, so that the relative orientations of the visible galaxies and of the radio structures could be used for studies of the source-collimation mechanism [following the work of Mackay (1971) and of Bridle and Brandie (1973)]. Identifications with faint (>18^m) or circular-looking galaxies were therefore given lower priority in the subsequent radio observations.

Given the relatively small dispersion in optical luminosity of elliptical radio galaxies (e.g., Sandage 1972) the apparent-magnitude cutoff arising from our initial selection criterion biases our sample towards systems of low radio luminosity in comparison with, for example, a sample of radio galaxies from the 3CR survey. In this respect results from our sample should correspond more to the statistics of radio galaxies in a given local volume than would similar results from 3CR galaxies.

b) The Pencil-Beam Observations

In June 1974 the 641 "optically measurable" radio galaxy candidates were observed with the NRAO 300-ft (91-m) transit telescope using the three-feed system at 2.7 GHz (Kesteven *et al.* 1976) to determine their total flux densities and centroidal positions at this frequency; these observations also indicated whether the sources had structure or were confused on angular scales from ~2 to ~10 arcmin. The results for "unresolved" sources (<2 arcmin) were given by Bridle *et al.* (1977). About 500 of the sources observed at the 300-ft telescope had integrated flux densities >0.125 Jy and appeared to be confined to angular scales <5 arcmin which could usefully be mapped with the NRAO 4-element dual-frequency interferometer (parameters in Table I).

c) The Interferometric Observations

Four interferometer configurations containing baselines from 0.1 km to 35.3 km were used at 2.7 GHz and 8.1 GHz between March 1974 and November 1975 (the journal of observations is given in Table II). The initial baselines of <0.3 km were valuable in establishing preliminary (accuracy ~5 arcsec) radio positions and gross angular extents of the sources. These observations, in some cases supplemented by the associated ~1.9-km baselines, allowed us to remove from the sample about 150 sources which were in fact not identified with optically measurable elliptical galaxies. (The identifications of these sources will be given in a later paper in this series.)

TABLE II. Journal of observations.

25–30 Jan 1974	0.8, 1.9, 2.7 km
14–18 Mar 1974	0.2, 1.9, 2.1 km
20 Aug–2 Sept 1974	0.1, 1.8, 1.9 km
22 Jan–2 Feb 1975	0.3, 1.2, 1.5 km
31 Mar–10 Apr 1975	0.9, 1.8, 2.7 km + 35 km
26 Oct–9 Nov 1975	0.6, 2.1, 2.7 km + 35 km

In order to determine the main features of the radio structures of the remaining ~350 radio galaxies using only a modest amount of observing time, each source was subsequently observed for 10 min at each of three or four hour angles with only those interferometer configurations for which it appeared that maximum information would be obtained. In this way partial synthesis maps were obtained for structures whose angular scales range from ~5 to ~300 arcsec, the data for each source being taken mainly on those baselines at which it produced appreciable signal. In most cases the synthesis proved to be of sufficient quality to define not only the angular extent and orientation of the source but also the major features of its morphology.

For a significant number of extended (>15 arcsec) sources there was signal at the longest baselines indicating the presence of a small-diameter radio component. All sources showing evidence of small-diameter components brighter than ~50 mJy at 2.7 or 8.1 GHz on the initial reductions of data from the 2.7-km baseline were specially observed on the three ~35-km baselines, generally for 10 min at each of five hour angles chosen to optimize the (u,v) coverage. During these 35-km baseline observations, gain and phase calibrations were made every 20 min. The calibrators were chosen as close in the sky as possible to the program sources in order to minimize the atmospheric phase fluctuations remaining after calibration.

As the areas of sky covered by extended sources may contain several optical objects, optical identifications can remain uncertain unless one of these objects itself proves to be a radio source, increasing the probability that it is the parent object of the entire source (see Sec. III below). For this reason we observed many sources at long baselines even if previous work had detected only large-scale structure. Most sources were observed for a total (all configurations) of ~2 h; the resulting point-source detection level at both 2.7 and 8.1 GHz is usually between 0.005 and 0.015 Jy. For sources whose overall extent exceeds ~20 arcsec the resolution was usually sufficient to distinguish high-brightness small components from the finer structure in the (sometimes complex) lower-brightness regions of the source.

d) Data Reduction

The NRAO interferometer data were calibrated in the usual manner. The gain and phase characteristics of

© American Astronomical Society • Provided by the NASA Astrophysics Data System

1978AJ.....83..704B

each correlator were generally monitored at least once per hour using unresolved calibration sources. At 2.7 GHz the flux-density scale was normalized to that of Bridle *et al.* (1977) by observing compact sources which did not vary during the 2-yr flux-density monitoring program of Kesteven *et al.* (1976). This ensured that the flux densities observed at the interferometer were on the same scale as the "zero-spacing" flux densities observed at the 300-ft telescope. At 8.1 GHz few nonvariable sources are sufficiently unresolved to be useful as phase calibrators, so a self-consistent scale was established for each observing session by relating the flux densities of known variable sources (a) to those of apparently flux-stable calibrators and (b) to a record of their 8.1-GHz "light curves" complied from the data of many observers at the NRAO interferometer by L. Blankenship and C. Williams. Phase calibrations at both frequencies were made using precise positions measured by C. M. Wade, K. Johnston, and C. Williams (unpublished).

Radio maps were made from the calibrated data using the normal Fourier methods. The details of how a "best" radio map was obtained for each field depend on the specifics of each source [overall angular size, complexity, amount and (u,v)-plane coverage of the data]. For the sources presented here we generally employed a three-step process. First, the overall size and structure were determined using only the shorter spacings at 2.7 GHz. Second, a map of the structure was prepared using a CLEAN procedure (Högbom 1974) to reduce the effects of sidelobes in the map. Careful planning of the observations and choice of the map areas to be CLEANed decreased the ambiguities associated with the CLEAN algorithm despite the relatively high sidelobe levels associated with partial synthesis data. A typical dynamic range for these maps was 10:1.

Our sensitivity to small-diameter components was enhanced by the third stage of data processing, in which the data were mapped and CLEANed using only the *outer* spacings at 2.7 and 8.1 GHz to emphasize fine structure in the sources. The small-diameter components reported here were most prominent on these high-resolution outer-spacing maps, which discriminate against contributions from the extended structure. In most cases the positions and flux densities of the small components were obtained by fitting Gaussian models to the long-spacing data using the high-resolution maps to guide the choice of initial model parameters. In some cases the parameters of the small components were determined by fitting more complex models to the large and fine-scale structures simultaneously. The combination of these procedures allows us, in favorable circumstances, to detect small components contributing as little as 1% of the total source intensity.

Most of the 35-km baseline observations were made during a period of excellent atmospheric phase stability in October and November 1975, and proved to be of sufficient quality to justify making synthesis maps at ~0.5 arcsec resolution (2.7 GHz) and 0.15 arcsec resolution (8.1 GHz) using the 2.7- and 35-km baselines. These maps were CLEANed and used to provide initial estimates of parameters for fits of Gaussian models to the 35-km data. Final positions, flux densities, and sizes of the more intense small-diameter components have been derived from these models.

III. RESULTS

a) The Small-diameter Components

Table III summarizes the radio results for the 48 small components. Column 1 gives the source name (IAU convention). Columns 2 and 3 give the observed radio position and its errors in each coordinate. The positions are generally weighted means of those found at 2.7 and 8.1 GHz using data from the longer Green Bank baselines. If the small component was partly confused with larger-scale structure at 2.7 GHz, the position is from the higher-resolution 8.1-GHz data only. Columns 4 and 5 give the 2.7- and 8.1-GHz flux densities for the small components, with their associated errors. Column 6 gives data (normally upper limits) on the fitted equivalent Gaussian diameters of the small components. Limits below 1 arcsec are derived from the observations on the 35-km baselines. A few components have definitely been resolved on scales between 0.2 and 2 arcsec; details of their fine structure are given in the notes following the Table.

Column 7 codifies the morphological relationship of the small-diameter component to the overall structure using the scheme shown in Fig. 1. If a prominent small component lies near the center of the overall structure, we assign code T or C. T denotes that the overall structure is basically bifurcated along its major axis of extension, so that the small component is the middle feature of the TRIPLE structure (the triple need not be collinear). C denotes that the extended emission is not clearly (or *uniquely*) bifurcated, so the small component is the

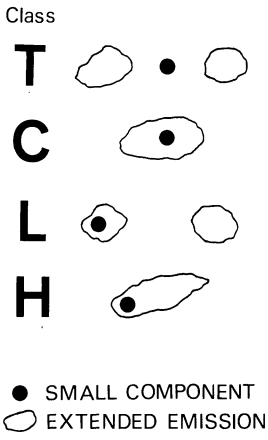

FIG. 1. Classification of relationship of small-diameter component to the overall structure. See Table III, Column 7 and Section III*a*.

© American Astronomical Society • Provided by the NASA Astrophysics Data System

1978AJ.....83..704B

TABLE III. Radio parameters of small components.

Source name	R.A. (1950)	Dec (1950)	S(2.7) Jy	S(8.1) Jy	Diam arcsec	Radio class	% Flux	Notes
0043+201	00 43 50.66	+20 11 42.3	0.019	0.018	<3	T	5.8	1
	0.04	0.7	0.011	0.007				
0055+300	00 55 05.64	+30 04 56.8	0.507	0.600	<0.1	T	33.8	2
	0.02	0.2	0.015	0.030				
0104+321	01 04 39.19	+32 08 44.5	0.072	0.112	<0.2	T	2.1	3
	0.03	0.3	0.014	0.025				
0109+492	01 09 04.94	+49 12 40.7	0.022	<0.020	≤4	T	1.8	4
	0.04	0.4	0.004					
0158+293	01 58 43.36	+29 19 17.4	<0.020	0.012	≤2	C(T)	<2.8	5
	0.02	0.4		0.004				
0206+355	02 06 39.33	+35 33 42.1	0.091	0.115	<0.2	C	6.5	6
	0.02	0.2	0.008	0.014				
0220+427	02 20 01.71	+42 45 55.0	0.225	0.158	<0.2	T(C)	4.3	7
	0.04	0.4	0.020	0.010				
0309+390	03 09 12.51	+39 05 15.9	<0.050	0.035	<2	T	<4.5	8
	0.04	0.5		0.010				
0331+391	03 31 00.94	+39 11 23.7	0.245	0.197	0.3	C	34.0	9
	0.02	0.2	0.011	0.021				
0349+212	03 49 45.18	+21 17 15.8	0.027	0.020	<2	T	7.5	10
	0.04	0.3	0.012	0.003				
0623+264	06 23 48.20	+26 25 10.6	0.151	0.170	<0.1	L(H)	15.1	11
	0.02	0.3	0.019	0.011				
0642+214	06 42 24.66	+21 25 02.2	0.470	0.370	<0.1	T	29.4	12
	0.02	0.2	0.016	0.030				
0652+426	06 52 37.11	+42 40 58.6	0.217	0.174	<0.2	T	32.9	
	0.02	0.2	0.016	0.011				
0712+534	07 12 42.17	+53 28 30.7	0.054	0.034	≤2	T	5.9	
	0.03	0.2	0.014	0.010				
0714+286	07 14 48.04	+28 40 35.4	<0.026	0.027	<2	T	<4.6	13
	0.02	0.3		0.004				
0755+379	07 55 09.07	+37 55 20.9	0.176	0.191	<0.1	T	10.1	14
	0.03	0.2	0.007	0.022				
0844+319	08 44 54.25	+31 58 13.5	0.036	0.029	<2	T	5.1	15
	0.03	0.3	0.007	0.007				
0917+458	09 17 50.67	+45 51 43.6	0.037	0.040	<2	T	0.8	16
	0.02	0.2	0.010	0.007				
1003+351	10 03 05.36	+35 08 48.3	2.092	0.858	0.8	T	59.8	17
	0.02	0.2	0.067	0.079				
1040+317	10 40 31.13	+31 46 50.6	0.052	0.041	<2	C	10.4	18
	0.02	0.3	0.005	0.004				
1113+295	11 13 53.57	+29 31 40.0	0.031	0.040	≤0.2	T	2.4	19
	0.03	0.4	0.008	0.010				
1123+203	11 23 21.20	+20 22 24.2	0.253	0.217	<0.2	L(H)	43.6	20
	0.02	0.2	0.021	0.023				
1140+217	11 40 21.37	+21 45 49.6	0.035	0.019	<3	T	8.8	21
	0.05	0.6	0.008	0.010				
1142+198	11 42 29.57	+19 53 02.6	0.258	0.220	<0.1	H(C)	8.6	22
	0.03	0.4	0.011	0.030				
1151+295	11 51 37.73	+29 32 57.5	0.052	0.056	<0.2	L	6.0	23
	0.03	0.3	0.010	0.009				
1316+299	13 16 43.15	+29 54 19.5	0.025	0.028	<2	T(C)	3.2	
	0.03	0.3	0.004	0.005				
1322+366	13 22 35.33	+36 38 18.6	0.060	0.067	<0.2	T	9.7	24
	0.03	0.3	0.010	0.010				
1346+268	13 46 33.95	+26 50 27.8	0.085	0.041	<0.2	T(C)	18.5	
	0.02	0.2	0.016	0.007				
1350+316	13 50 03.24	+31 41 33.1	2.400	1.030	2	?	82.8	25
	0.02	0.2	0.080	0.040				
1420+198	14 20 41.50	+19 48 54.6	0.578	0.189	1.4	L	29.6	26
	0.02	0.2	0.025	0.032				
1446+206	14 46 32.88	+20 38 03.0	0.300	0.089	1	L	57.7	27
	0.02	0.2	0.100	0.010				
1452+166	14 52 00.63	+16 36 34.6	0.208	0.199	<0.1	?	20.8	
	0.02	0.2	0.005	0.009				
1502+262	15 02 46.88	+26 12 34.8	0.087	0.052	<0.2	T	2.8	28
	0.03	0.2	0.005	0.006				
1511+263	15 11 30.81	+26 18 39.8	0.200	0.074	2.2	C	8.7	29
	0.02	0.3	0.014	0.020				
1553+245	15 53 56.19	+24 35 32.6	0.056	0.042	<0.2	T(C)	35.0	30
	0.02	0.2	0.009	0.010				
1557+708	15 57 41.20	+70 49 51.2	0.022	0.040	<0.2	C	2.9	31
	0.04	0.3	0.006	0.006				
1626+396	16 26 55.33	+39 39 36.6	0.168	0.120	<0.1	T	12.9	32
	0.02	0.2	0.013	0.013				
1658+302	16 58 48.94	+30 12 33.7	0.072	0.074	<2	T(C)	16.4	33
	0.03	0.3	0.008	0.005				
1744+557	17 44 00.54	+55 43 25.2	0.211	0.213	<0.1	T(C)	35.2	
	0.03	0.2	0.020	0.020				

© American Astronomical Society • Provided by the NASA Astrophysics Data System

1978AJ.....83..704B

[TABLE III (continued)]

Source name	R.A. (1950)	Dec (1950)	S(2.7) Jy	S(8.1) Jy	Diam arcsec	Radio class	% Flux	Notes
1759+211	17 59 40.56	+21 09 24.8	0.030	0.018	<2	T	7.1	
	0.03	0.6	0.010	0.006				
1833+326	18 33 11.99	+32 39 18.2	0.212	0.173	<0.1	T(C)	6.1	34
	0.02	0.2	0.025	0.011				
1834+196	18 34 29.53	+19 41 11.3	0.181	0.154	<0.1	T	16.5	
	0.03	0.2	0.013	0.011				
1842+455	18 42 35.45	+45 30 21.4	0.055	0.040	<0.2	T	1.7	35
	0.03	0.2	0.011	0.010				
1845+797	18 45 37.90	+79 43 06.6	0.430	0.600	<0.1	T	6.6	36
	0.05	0.2	0.030	0.034				
1940+504	19 40 25.62	+50 28 37.5	0.043	0.023	<1	C	3.2	37
	0.02	0.2	0.010	0.005				
2229+391	22 29 07.58	+39 06 04.2	0.038	0.042	<0.2	T	1.6	38
	0.04	0.5	0.007	0.008				
2234+386	22 34 34.10	+38 37 42.5	0.041	0.026	<2	T	5.9	39
	0.02	0.3	0.009	0.007				
2335+267	23 35 58.98	+26 45 16.3	0.278	0.235	<0.1	T(C)	6.6	40
	0.03	0.3	0.014	0.012				

Notes to Table III

(1) 0043+201: Owen *et al.* (1977) show a 2.7-GHz map.
(2) 0055+300: Bridle *et al.* (1976) give details of the large-scale structure. Fanti *et al.* (1976) map the inner structure at 1.4 GHz.
(3) 0104+321: 3C 31; Macdonald *et al.* (1968) show a 408-MHz map. Schilizzi (1976) finds 0.15 Jy in 0.01 arcsec at 8.1 GHz.
(4) 0109+492: 3C 35; Mackay (1969) shows a 408-MHz map. Bridle *et al.* (1972b) suggest that a nearby source BDFL 0110+495 (not included in our LAS estimate) may be related.
(5) 0158+293: The small component is 0.016 Jy at 4.9 GHz (Fomalont and Bridle 1978).
(6) 0206+355: Pooley and Henbest (1974) show a 5-GHz map.
(7) 0220+427: 3C 66(B); mapped by Northover (1973) at 1.4, 2.7, and 5.0 GHz.
(8) 0309+390: Studied in detail by Adams and Rudnick (1977).
(9) 0331+391: The small component may contain a <0.1 arcsec core with ~0.13 Jy at both 2.7 and 8.1 GHz. The ~0.3 arcsec structure may be elongated along p.a. 120° ± 30°. Fanti *et al.* (1977) show a 5-GHz map.
(10) 0349+212: Owen *et al.* (1977) show a 2.7-GHz map.
(11) 0623+264: Our position for the small component is from the 8.1-GHz data only.
(12) 0642+264: 3C 166; Kesteven *et al.* (1976) found the total intensity varied at 2.7 GHz; the variations probably arise in the small component found here.
(13) 0714+286: The small component is 0.017 Jy at 4.9 GHz (Fomalont and Bridle 1978).
(14) 0755+379: Emission on a scale of several arc sec surrounds the small component (see Fig. 3b). Fanti *et al.* (1977) show 1.4- and 5-GHz maps; there may be jets connecting the outer emission to the small source.
(15) 0844+319: Mapped at 5 GHz by van Breugel and Miley (1977).
(16) 0917+458: 3C 219; discussed in detail by Turland (1975), whose 5-GHz map shows a "jet" South–West of the small component.
(17) 1003+351: 3C 236; the large-scale structure has the largest linear size of any well-mapped source (Willis *et al.* 1974). The small core was mapped at 2.7 and 8.1 GHz by Fomalont and Miley (1975). Preuss *et al.* (1977) find 0.08 Jy in <0.002 arcsec at 5 GHz.
(18) 1040+317: Fanti *et al.* (1977) show a 5-GHz map.
(19) 1113+295: Riley (1975) and Fanti *et al.* (1977) show 5-GHz maps. Owen *et al.* (1977) show a 2.7-GHz map.
(20) 1123+203: There is possibly structure on scales ~1 to ~2 arcsec around the small component, containing a further ~0.15 Jy at 2.7 GHz and ~0.07 Jy at 8.1 GHz; see also Fig. 3d.
(21) 1140+217: The 4C position (4C 21.33) is lobe-shifted early.
(22) 1142+198: 3C 264; mapped at 2.7 and 5 GHz by Northover (1976). We find ~0.15 Jy in ~2 arcsec near the small component, in agreement with the total ascribed to a compact component by Northover.
(23) 1151+295: A further ~0.04 Jy is present in ~3 arcsec structure near the small component (see Fig. 3f).
(24) 1322+366: Fanti *et al.* (1977) show a 5-GHz map.
(25) 1350+316: 3C 293; our data confirm the reality of the North–West component on the 5-GHz map of Branson *et al.* (1972) and suggest that there is further large-scale emission between this component and the galaxy (see Fig. 4d).
(26) 1420+198: 3C 300; Riley and Pooley (1975) give a 5-GHz map.
(27) 1446+206: The small component was resolved on the 35-km baselines at both 2.7 and 8.1 GHz; the overall structure was mapped at 5 GHz by Pooley and Henbest (1974).
(28) 1502+262: 3C 310; discussed in detail by van Breugel and Miley (1977).
(29) 1511+263: 3C 315; studied in detail by Northover (1976), who gave a size of 3.3 arc sec for the small component. We find this component elongated along p.a. 173° ± 20°.
(30) 1553+245: Fanti *et al.* (1977) show a 5-GHz map.
(31) 1557+708: The extended source was heavily resolved even at 100 m spacings. The structure was classified C (not uniquely bifurcated) because of the missing flux density and of the ambiguity about how much of the mapped emission is physically related.
(32) 1626+396: 3C 338; mapped at 2.7 GHz by Rudnick and Owen (1977) and at 5 GHz by Jaffe and Perola (1974). Preuss *et al.* (1977) indicate that the small component is <~0.001 arcsec at 5 GHz.
(33) 1658+302: The 4C position (4C 30.31) is lobe-shifted early. The extended emission contains about 400 mJy at 2.7 GHz in structure approximately 120 by 40 arcsec elongated in p.a. 65° ± 20°. The morphology of this emission is uncertain.
(34) 1833+326: 3C 382; mapped at 5 GHz by Riley and Branson (1973) and Fanti *et al.* (1977); Preuss *et al.* (1977) find <0.1 Jy in 0.001 arcsec at 5 GHz.
(35) 1842+455: 3C 388; Pooley and Henbest (1974) show a 5-GHz map.
(36) 1845+797: 3C 390.3; studied in detail by Harris (1972). Preuss *et al.* (1977) indicate that the small component is <0.001 arcsec.
(37) 1940+504: 3C 402; the region was mapped by Riley and Pooley (1975) and by Miley and van der Laan (1973).
(38) 2229+391: 3C 449; Fanti *et al.* (1977) show 0.6- and 5-GHz maps.
(39) 2234+386: Our observations were partly confused by WK459 = 2235+385 (Windram and Kenderdine 1969). A 2.7-GHz map will be shown by Rudnick and Adams (1978, in preparation).
(40) 2335+267: 3C 465; the large-scale structure was mapped by Macdonald *et al.* (1968), Miley and van der Laan (1973) and Riley and Branson (1973). Preuss *et al.* (1977) find the core extended 0.0013 arcsec in p.a. 116° at 5 GHz.

© American Astronomical Society • Provided by the NASA Astrophysics Data System

1978AJ.....83..704B

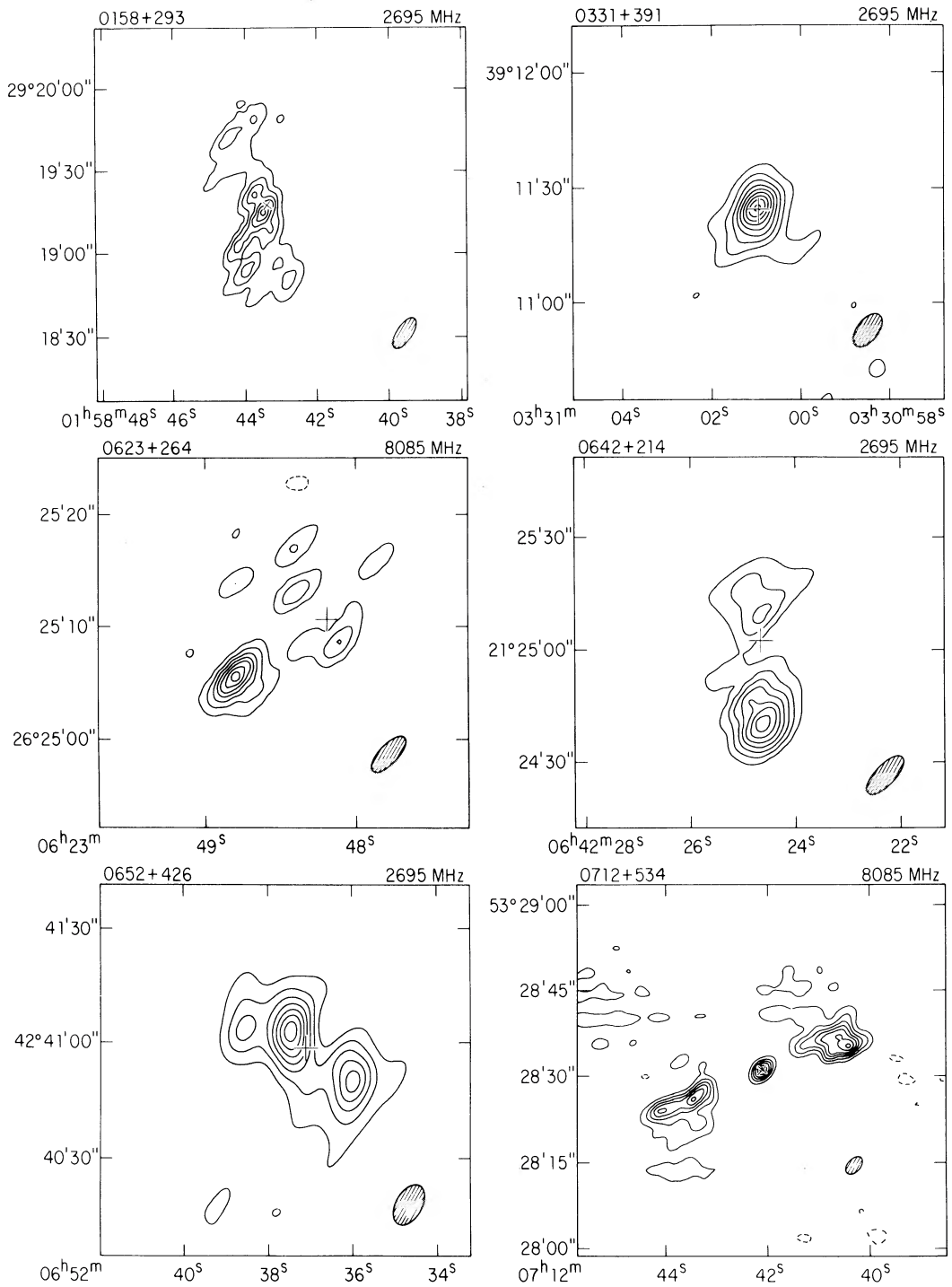

FIG. 2. (a) 0158+293: Each contour level is 18.3 mJy/beam. The small-diameter component has not been substracted. (b) 0331+391: Each contour level is 15.0 mJy/beam. A 245 mJy small-diameter component has been subtracted. Fanti *et al.* (1977) show a 5-GHz map with the extended emission more elongated in the North–South direction. (c) 0623+264: Each contour level is 11.9 mJy/beam. A 151 mJy small-diameter component has been subtracted. (d) 0642+214: Each contour level is 33.6 mJy/beam. A 470 mJy small-diameter component has been subtracted. (e) 0652+426: Each contour level is 13.6 mJy/beam. A 217 mJy small-diameter component has been subtracted. (f) 0712+534: Each contour level is 5.4 mJy/beam. The small-diameter component has not been subtracted.

© American Astronomical Society • Provided by the NASA Astrophysics Data System

1978AJ.....83..704B

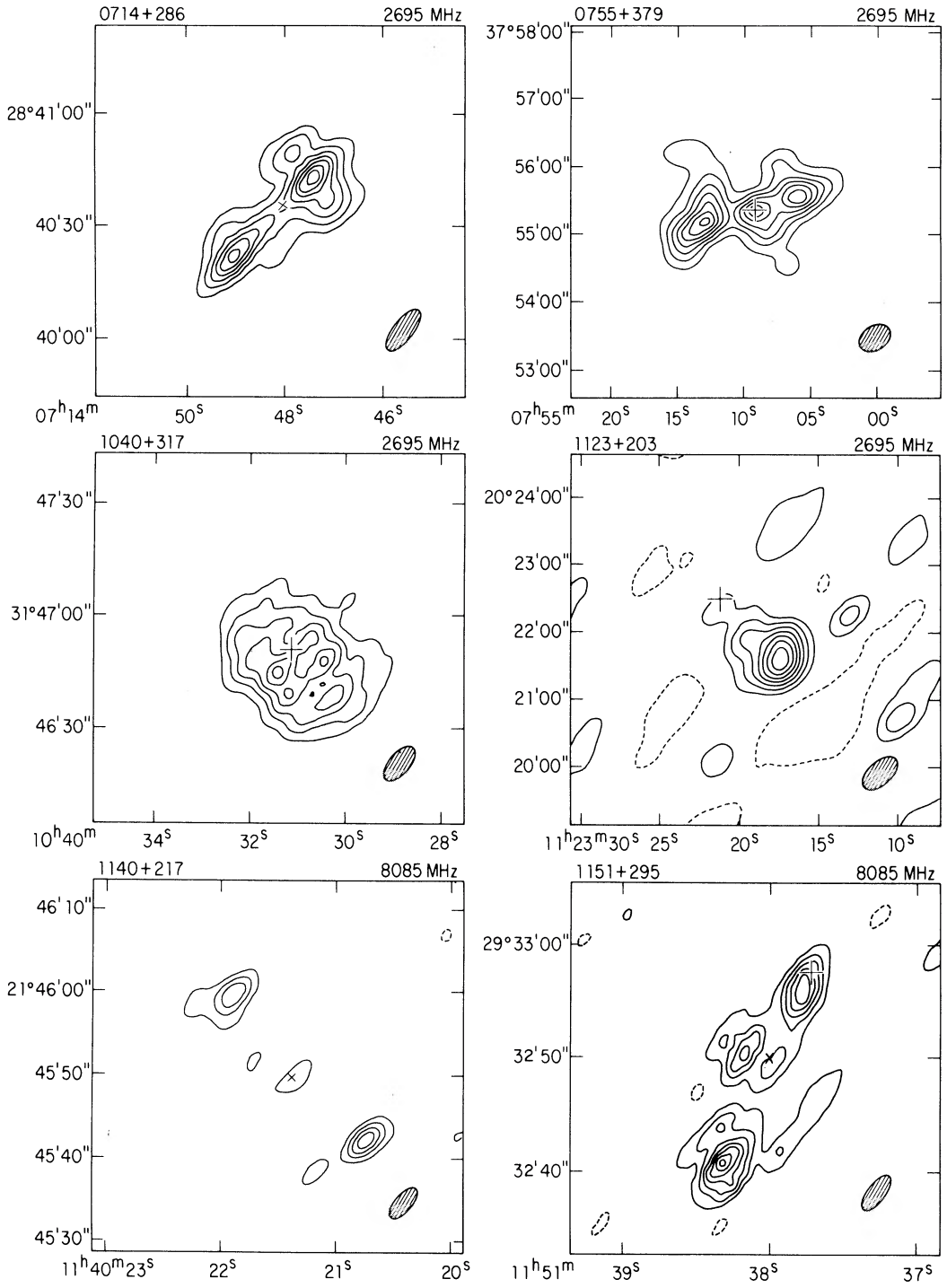

FIG. 3. (a) 0714+2-86: Each contour level is 18.2 mJy/beam. The small-diameter component has not been substracted. (b) 0755+379: Each contour level is 30.9 mJy/beam. A 176 mJy small-diameter component has been subtracted. Fanti *et al.* (1977) show 1.4- and 5-GHz maps in good agreement with this synthesis. (c) 1040+317: Each contour level is 9.1 mJy/beam. A 52 mJy small- diameter component has been subtracted. A 5-GHz map by Fanti *et al.* (1977) shows essentially similar features. (d) 1123+203: Each contour level is 9.1 mJy/beam. A 253 mJy small-diameter component has been subtracted. (e) 1140+217: Each contour level is 4.0 mJy/beam. The small-diameter component has not been subtracted. (f) 1151+295: Each contour level is 4.7 mJy/beam. A 52 mJy small-diameter component has been subtracted.

© American Astronomical Society • Provided by the NASA Astrophysics Data System

1978AJ.....83..704B

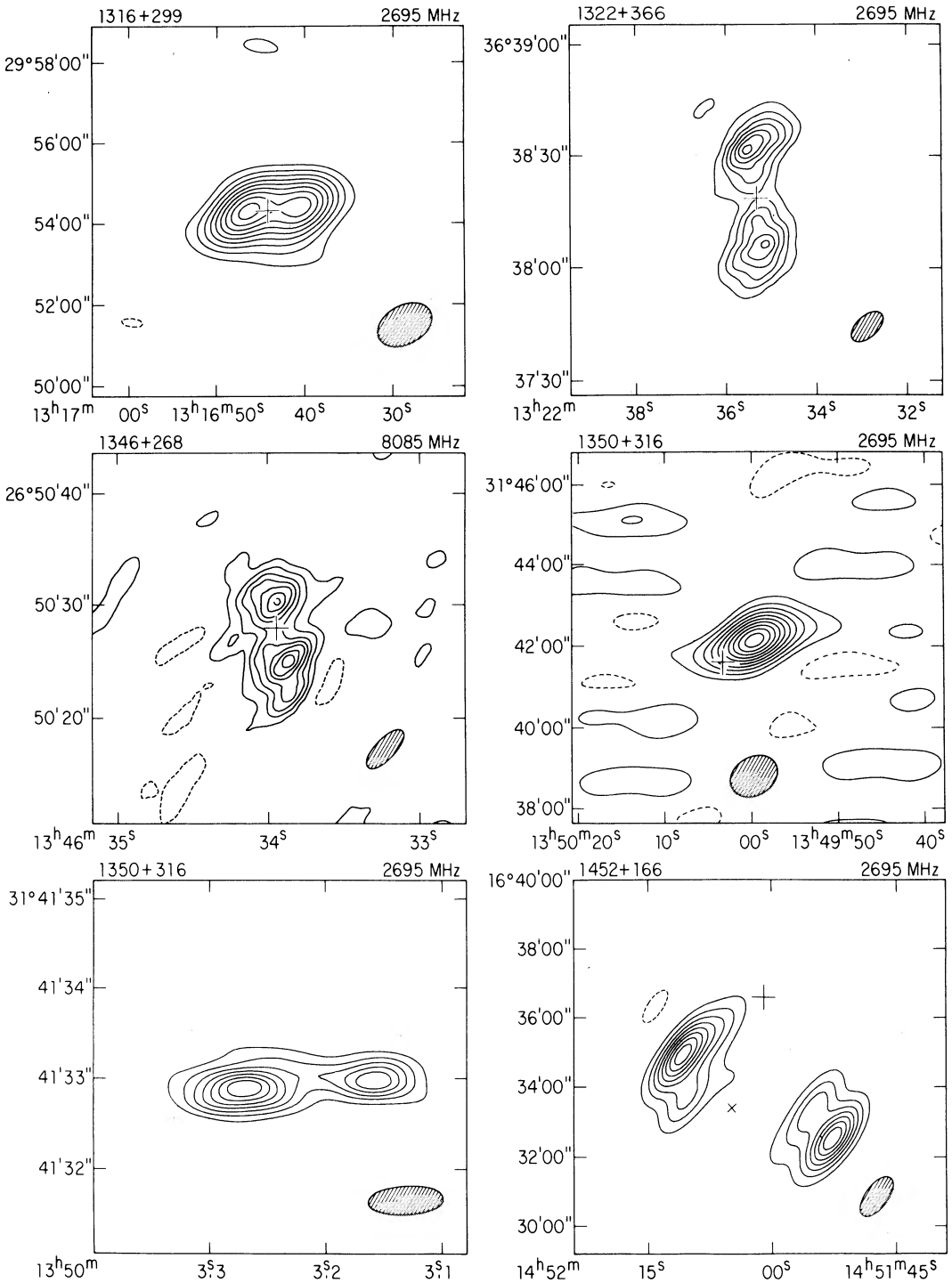

FIG. 4. (a) 1316+299: Each contour level is 32.8 mJy/beam. A 25 mJy small-diameter component has been substracted. (b) 1322+366: Each contour level is 14.5 mJy/beam. A 60 mJy small-diameter component has been subtracted. The map is in good agreement with a 5-GHz map by Fanti *et al.* (1977). (c) 1346+268: Each contour level is 2.4 mJy/beam. An 85 mJy small-diameter component has been subtracted. (d) 1350+316 LOW RESOLUTION: Each contour level is 32.0 mJy/beam. A 2400 mJy small-diameter component has been subtracted. (e) 1350+316 HIGH RESOLUTION (beam 0.26 by 0.64 arcsec): Each contour level is 79.1 mJy/beam. This map shows only the small-diameter component; the size and position angle are in good agreement with the lower-resolution model of Jenkins *et al.* (1977). (f) 1452+166: Each contour level is 21.4 mJy/beam. A 208 mJy small-diameter component coincident with a $18\overset{m}{.}3$ optical object has been subtracted (+). The identification of Schilizzi (1975), a 15^m galaxy, is shown by the (x).

© American Astronomical Society • Provided by the NASA Astrophysics Data System

1978AJ.....83..704B

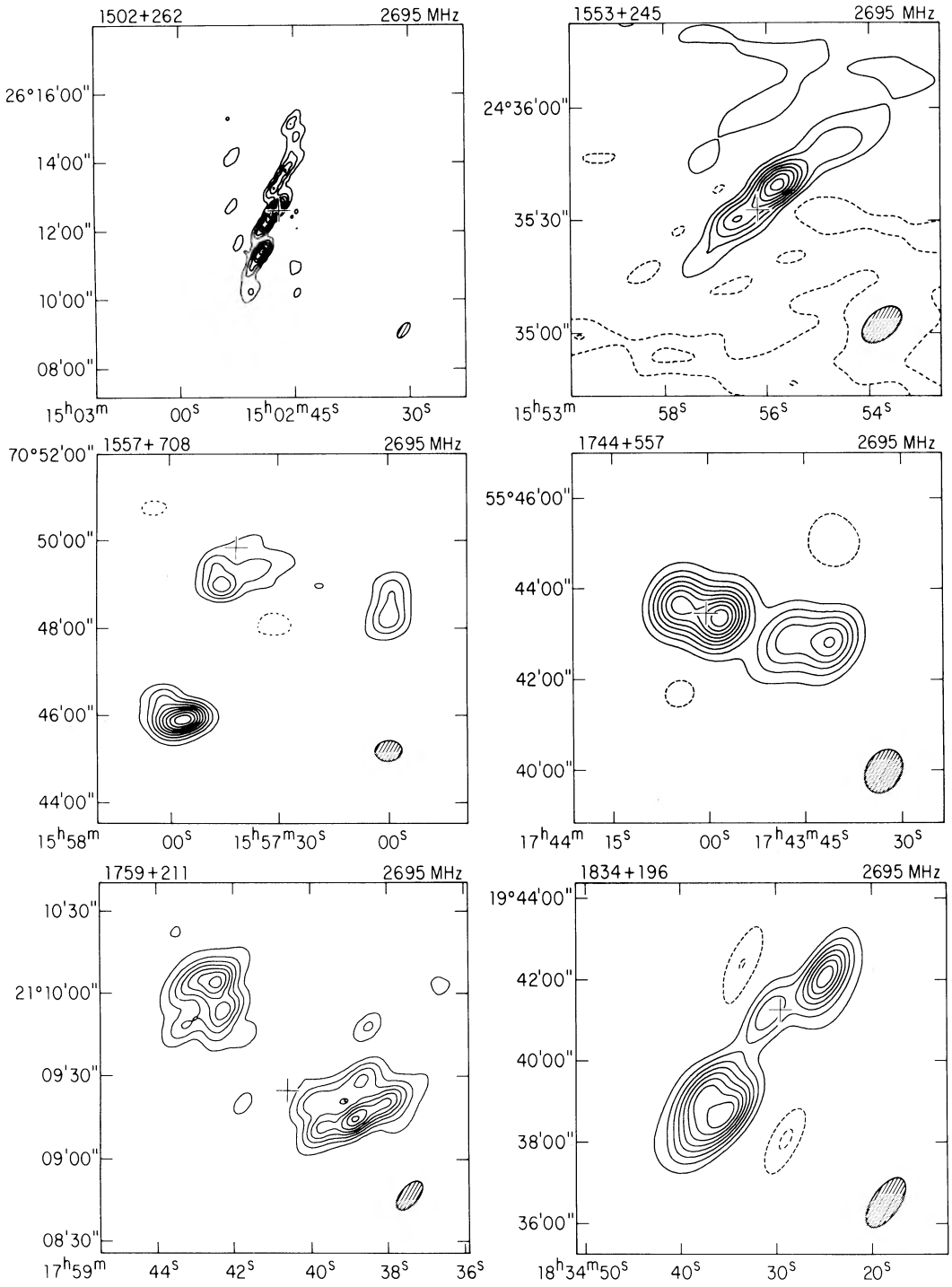

FIG. 5. (a) 1502+262: Each contour level is 50.0 mJy/beam. An 87 mJy small-diameter component has been substracted. A further 500 mJy is present in larger-scale structure whose morphology is indeterminate from our data. (b) 1553+245: Each contour level is 2.8 mJy/beam. A 56 mJy small-diameter component has been subtracted. The map is in good agreement with the 5-GHz map by Fanti *et al.* (1977). (c) 1557+708: Each contour level is 7.8 mJy/beam. A 22 mJy small-diameter component has been subtracted. (d) 1744+557: Each contour level is 4.3 mJy/beam. A 211 mJy small-diameter component has been subtracted. (e) 1759+211: Each contour level is 6.5 mJy/beam. A 30 mJy small-diameter component has been subtracted. (f) 1834+196: Each contour level is 28.0 mJy/beam. A 181 mJy small-diameter component has been subtracted.

© American Astronomical Society • Provided by the NASA Astrophysics Data System

1978AJ.....83..704B

CORE of a "core-halo" or "complex" structure. If the only small component lies near one end of the overall structure, we assign code L or H on a similar basis. L denotes that the overall structure appears bifurcated as above, so that the small component appears to be in one LOBE of the structure. H denotes that the overall structure does not appear bifurcated along its major axis, so that the small component appears to be at the HEAD of a narrow "head-tail" structure. Because published work (e.g., Pooley and Henbest 1974; Riley and Pooley 1975) indicates that centrally-located small components are more likely to be physically associated with the optical identifications of powerful radio sources, *we have given priority to central components in classifying the structures of sources with both central and peripheral fine structure.* There are inevitable transition cases which are hard to classify on this idealized scheme (see Sec. III*d* below); for these the most likely alternative classification is given in parentheses in Column 7.

Column 8 gives the 2.7-GHz flux density of the small component as a percentage of the total flux density at this frequency. The total flux densities have been derived mainly from our pencil-beam observations (Sec. II*b*) with occasional reference to lower-resolution measurements and to the published total spectrum (for sources more than 5 arcmin in overall extent). An asterisk in Column 9 indicates that further details about the source are given in a footnote in Table III.

b) Maps of the Overall Structures

Figures 2–5 give CLEANed contour maps showing the structure of the large-scale emission for those sources for which no comparable data had been published by September 1977. (The notes to Table III give references to published maps of the other sources.) In each case we have selected the map frequency and angular resolution which best displays the overall structure. If the small-diameter component contains a large fraction of the total intensity, it has been deleted from these maps to clarify the presentation of the extended structure and its position is shown by a + symbol. Such deletions were made by vectorially subtracting the contribution of the fitted component from the amplitudes and phases observed on each baseline, and then repeating both the Fourier-inversion and CLEAN stages of data processing (Sec. II*c*). In several maps an x indicates the position of a small component not subtracted and/or the position of a galaxy. In all maps the CLEAN synthesized beam is illustrated by the cross-hatched ellipse (FWHM).

Since Figs. 2–5 were prepared, partial synthesis maps of several of the sources were published by Fanti *et al.* (1977). The agreement between their maps and ours is generally excellent. Given the different configurations of the Westerbork and NRAO instruments this agreement demonstrates the success of the partial synthesis technique when care is taken over baseline selection and the CLEAN reductions.

c) Incidence of Small Components

About 150 sources in our overall sample (Sec. I *a*) have angular extents >20 arcsec, $\delta > +15°$ and sufficient observations for us to detect any small component at the ~1% level. We have found such components in ~30% of this sample; although the sample is by no means uniform, it is evident that at least a substantial minority of the extended radio galaxies contains small components with a few percent or more of the total 2.7-GHz flux density. Studies of nearby galaxies at higher frequencies have shown the incidence of all classes of small components in complete volume-limited samples to be ~50% (Colla *et al.* 1975a) or higher (Schilizzi 1976), possibly limited only by instrumental sensitivity.

d) Small Components in Asymmetric Locations

Most of the classification ambiguities in Table III are between classes T and C and result from ambiguities in whether or how the extended emission is bifurcated around an essentially central small component. These ambiguities may be related to barely-resolved bridges or jets between the major components or to lack of strong high-brightness substructure in the outer parts of complex sources. In 0623+264, 1123+203, 1142+198, and 1350+316, however, the ambiguity is associated with asymmetric location of the small component in an extended structure whose morphology is unclear; in 1452+166 the overall structure is clearly double, but the small component may not be related to the extended source (Sec. IV *b*).

Before subtraction of the small components, 0623+264 and 1123+203 appear to be flux-asymmetric doubles, but in both cases most of the intensity in what is ostensibly the brighter "lobe" is concentrated in the small component. The emission remaining after subtraction of the small component (Figs. 2c and 3d) appears weakly bifurcated; these systems may be asymmetric doubles or "head–tails" in which the tail brightens away from the head. We favor the former interpretation but retain both possibilities in the L(H) classification assigned in Table III. In both cases the mapped flux density accounts for the total detected in the pencil-beam observations within errors.

For 1142+198 our 2.7-GHz map, the 408-MHz map (Macdonald *et al.* 1968), and the 1.4-GHz map (Högbom and Carlsson 1974) support classification of the overall structure as H on the evidence of the displacement of the source centroid from the small component and of the brightness gradient away from this component. The 2.7-GHz map by Northover (1976), however, shows emission on the other side of the small component suggestive of structure akin to the "wide-angle" tails discussed by Owen and Rudnick (1976). The small component may be the core of a structure whose symmetry changes with frequency due to spectral-index variations across the source; the apparent size of this

© American Astronomical Society • Provided by the NASA Astrophysics Data System

1978AJ.....83..704B

source is known to vary with frequency (e.g., Northover 1976).

The source 1350+316 is exceptional in several respects. 80% of the emission is located in the small component (Fig. 4e), the highest proportion in any source in the sample. The extended emission has a large angular size and its detailed morphology is difficult to determine with our limited hour-angle sampling. A weak component ~90 arcsec North–West of the main source was reported by Mackay (1969) and by Branson *et al.* (1972). We confirm the presence of emission near this component and suggest that there is further large-scale emission between it and the small component (Fig. 4d). The structure of this large-scale emission is uncertain and it may extend South–East of the main component; the wide range of surface brightness and the low intensity of the extended emission result in large uncertainties in the CLEANed maps of the extended structure, so we do not classify the overall morphology in Table III.

IV. OPTICAL IDENTIFICATIONS

a) Identification Procedure

Transparent overlays were made for the *Palomar Sky Atlas* showing the positions of the small-diameter and extended radio components in each source. These overlays located the radio components on the *Sky Atlas* prints (using *Smithsonian Astrophysical Observatory Catalogue* stars as fiducial markers) to an rms accuracy of ~5 arcsec. Galaxies or groups of galaxies were found near the radio positions of the small components in each of the 41 structures classified as triple (T), complex (C) or head-tail (H) in Table III, and in the four structures classified L(H) or "?". Only in the three structures definitely classified L in Table III was the nearest optical image on the *Sky Atlas* prints significantly displaced from the position of the small component.

Precise optical positions were measured for all optical identification candidates suggested by the overlay inspection, except for those with optical positions quoted to better than ~1 arcsec in the literature. The positions were measured relative to reference stars from the AGK3 Catalog using the two-coordinate measuring engine and reduction procedure described by Bridle and Goodson (1977). Further details of the position measurements will be given in Paper III of this series (Goodson *et al.* 1978). In all 45 sources with structure classes other than L the centre of a galaxy coincides with the radio position of the small component to the accuracy expected from the combined optical and radio position errors (typically ~1 arcsec).

b) Identification Reliability

In the 45 sources where small radio components coincide with the centers of galaxies, the small components must be physically associated with the measured optical systems, for the probability of random coincidence to within ~1 arcsec between an arbitrary position and the center of a galaxy of any magnitude brighter than 19^m is only $\sim 2 \times 10^{-5}$ [based on galaxy counts at high galactic latitudes (Allen 1973)]. The question arises however: What is the probability that the small component/radio galaxy is randomly present in the same field as the extended radio structure?

There are three criteria which may be used to determine the reliability of an identification of a galaxy with a radio source. First, *the structural features of the source may provide morphological evidence for association with the galaxy.* In some cases—0055+300 (Bridle *et al.* 1976), 0220+427 (Northover 1973) and 0844+319 (van Breugel and Miley 1977)—the morphological evidence for association is unambiguous because the distant extended emission is linked by bridges or jets to the center of the optical identification. In other cases the position of a galaxy near the centroid of the radio emission, or along a well-defined major axis of the emission, provides weaker support for the identification.

Second, a galaxy lying in or near the radio structure may be so bright that *the a priori probability of the galaxy being situated randomly within the radio emission is very small.* Many published identifications rely on application of this criterion; however, extended radio sources may overlap the images of several galaxies of comparable apparent magnitude, especially within clusters or groups of galaxies. In the absence of a firm astrophysical basis for associating radio sources solely with the most luminous galaxies in groups or clusters, it is important to confirm identifications made on this "brightest-galaxy" criterion.

Third, an optical object lying in or near the radio structure may itself contain a small-diameter radio component which is so strong that *the a priori probability of the small radio component lying randomly within the extended emission is small.* With sensitive, high-resolution observations this criterion is becoming more useful. We have combined all three criteria to appraise the reliability of the identification of each source listed in Table III.

We first apply the third criterion using the 2.7-GHz source count presented by Fomalont *et al.* (1974) to estimate the probability that the small radio component lies by chance anywhere within the area of sky "covered" by the extended radio structure of each source. The area "covered" by the source was conservatively taken as a circular area whose angular radius is half the greatest angular distance between the 10% peak brightness contours on our 2.7 GHz map of the extended emission. As the small components in the 45 sources with T and C structures lie in the inner quarter of this area by definition, our probability estimates are conservative by a factor ~4 for most of the sources. Even with this generous assignment of the area covered by each source, only six small-diameter components (those in 0055+300, 0109+492, 0844+319, 1502+262, 1557+708, and 2229+391) have probabilities >1% of lying in the ex-

© American Astronomical Society • Provided by the NASA Astrophysics Data System

1978AJ.....83..704B

TABLE IV. Optical parameters of identifications.

Source	Opt name	R.A. (1950)	Dec (1950)	DRA	DDEC	Mag	z	Refs.
0043+201		00 43 50.73	+20 11 41.8	1.0	−0.5	15.7	0.1028	1,7,22
		0.03	0.7					
0055+300	NGC 315	00 55 05.60	+30 04 56.0	−0.5	−0.8	11.5	0.0167	2,8,23
		0.30	3.0					
0104+321	NGC 383	01 04 39.10	+32 08 43.3	−1.1	−1.2	11.7	0.0169	1,9,24
		0.03	0.4					
0109+492		01 09 04.94	+49 12 40.1	0.0	−0.6	14.7	0.0677	1,10,24
		0.04	0.4					
0158+293		01 58 43.49	+29 19 16.0	1.7	−1.4	16.2	0.1482	1,11,25
		0.04	0.4					
0206+355	VV6-5-88	02 06 39.30	+35 33 41.3	−0.4	−0.8	13.6	0.0374	1,12,26
		0.03	0.4					
0220+427	VV7-6-3	02 20 01.78	+42 45 54.6	0.8	−0.4	12.5	0.0215	3,13,27
		0.05	0.5					
0309+390		03 09 12.60	+39 05 15.6	1.0	−0.3	16.0	0.1610	1,14,28
		0.03	0.5					
0331+391	VV6-8-34	03 31 00.94	+39 11 23.5	0.0	−0.2	12.4	0.0209	1,15,23
		0.05	0.4					
0349+212		03 49 45.19	+21 17 16.2	0.1	0.4	16.6	0.1325	1,16,29
		0.04	0.4					
0623+264		06 23 48.27	+26 25 09.5	0.9	−1.1	16.4	(0.1140)	1,29
		0.07	0.4					
0642+214		06 42 24.66	+21 25 02.2	0.0	0.0	17.7	(0.1870)	1,24
		0.03	0.5					
0652+426		06 52 37.09	+42 40 58.7	−0.2	0.1	14.5	(0.0520)	1,30
		0.06	1.2					
0712+534		07 12 42.14	+53 28 30.9	−0.3	0.2	13.7	(0.0367)	4,31
		0.04	0.4					
0714+286		07 14 48.03	+28 40 35.9	−0.1	0.5	15.6	0.0830	1,11,30
		0.03	0.4					
0755+379	NGC 2484	07 55 09.07	+37 55 20.9	0.0	0.0	13.2	0.0433	1,17,25
		0.03	0.4					
0844+319	NGC 2402	08 44 54.30	+31 58 13.4	0.6	−0.1	14.0	0.0675	1,11,26
		0.03	0.4					
0917+458		09 17 50.66	+45 51 43.9	−0.1	0.3	17.2	0.1745	3,18,32
		0.05	0.5					
1003+351		10 03 05.37	+35 08 48.1	0.2	−0.2	16.1	0.0988	1,19,24
		0.03	0.2					
1040+317		10 40 31.18	+31 46 51.1	0.6	0.5	14.9	0.0360	1,8,23
		0.05	0.7					
1113+295	VV5-27-40	11 13 53.59	+29 31 40.3	0.3	0.3	14.6	0.0489	1,8,26
		0.03	0.3					
1123+203		11 23 21.20	+20 22 25.3	0.0	1.1	16.2	0.1316	1,11,29
		0.02	1.3					
1140+217		11 40 21.31	+21 45 50.7	−0.8	1.1	16.6	(0.1240)	1,33
		0.04	0.5					
1142+198	NGC 3862	11 42 29.64	+19 53 02.5	1.0	−0.1	13.6	0.0206	5,18,24
		0.07	1.0					
1151+295		11 51 37.97	+29 32 50.1	3.1	−7.4	19.4	0.3292	1,11,26
		0.04	0.5					
1316+299		13 16 43.17	+29 54 20.0	0.3	0.5	15.7	0.0728	1,11,26
		0.03	0.3					
1322+366	NGC 5141	13 22 35.34	+36 38 18.9	0.1	0.3	13.2	0.0176	1,12,26
		0.02	0.3					
1346+268	VV5-33-5	13 46 33.98	+26 50 27.8	0.4	0.0	14.6	0.0630	1,11,26
		0.04	0.3					
1350+316	VV5-33-12	13 50 03.20	+31 41 33.8	−0.5	0.7	14.1	0.0454	1,20,34
		0.03	0.6					
1420+198		14 20 40.10	+19 49 12.4	−19.8	17.8	19.0	(0.2900)	5,24
		0.07	1.0					
1446+206		14 46 33.12	+20 37 58.4	3.4	−4.6	19.3	0.2540	1,11,26
		0.05	0.4					
1452+166		14 52 00.63	+16 36 34.2	0.0	−0.4	18.3	(0.2290)	1,33
		0.02	0.5					
1502+262		15 02 46.94	+26 12 34.7	0.8	−0.1	16.1	0.0543	3,18,27
		0.04	0.5					
1511+263		15 11 30.82	+26 18 40.3	0.1	0.5	16.4	0.1086	1,18,27
		0.02	0.5					
1553+245		15 53 56.21	+24 35 32.9	0.3	0.3	14.8	0.0426	1,8,23
		0.04	0.4					
1557+708	VV12-15-38	15 57 41.25	+70 49 49.8	0.2	−1.4	12.6	(0.0226)	1,33
		0.08	0.4					
1626+396	NGC 6166	16 26 55.38	+39 39 36.6	0.6	0.0	12.3	0.0303	3,21,27
		0.04	0.5					
1658+302		16 58 48.97	+30 12 33.2	0.4	−0.5	14.1	(0.0435)	1,34
		0.02	0.4					

© American Astronomical Society • Provided by the NASA Astrophysics Data System

1978AJ.....83..704B

TABLE IV (continued)

Source	Opt Name	R.A. (1950)	Dec (1950)	DRA	DDEC	MAG	z	Refs.
1744+557	NGC 6454	17 44 00.58	+55 43 25.0	0.3	−0.2	13.2	0.0312	1,12,35
		0.03	0.4					
1759+211		17 59 40.50	+21 09 25.1	−0.8	0.3	15.5	(0.0800)	1,36
		0.03	0.7					
1833+326		18 33 11.99	+32 39 17.9	0.0	−0.3	14.0	0.0586	1,18,24
		0.02	0.4					
1834+196		18 34 29.47	+19 41 09.9	−0.8	−1.4	12.9	0.0166	1,12,37
		0.03	0.4					
1842+455		18 42 35.44	+45 30 21.7	−0.1	0.3	15.0	0.0917	3,18,27
		0.05	0.5					
1845+797		18 45 37.64	+79 43 06.1	−0.7	−0.5	15.6	0.0569	1,20,24
		0.11	0.4					
1940+504	VV8-36-3	19 40 25.65	+50 28 38.4	0.3	0.9	13.3	0.0247	6,10,38
		0.15	1.0					
2229+391	VV6-49-29	22 29 07.71	+39 06 04.4	1.5	0.2	12.7	0.0181	5,19,24
		0.09	1.0					
2234+386		22 34 34.08	+38 37 42.6	−0.2	0.1	15.1	(0.0670)	1,25
		0.05	0.4					
2335+267	NGC 7720	23 35 58.94	+26 45 16.4	−0.5	0.1	13.1	0.0301	1,18,24
		0.06	0.4					

Notes to Table IV

0309+390 Previously identified incorrectly with NGC 1233 (Aizu 1966; Caswell and Wills 1967).
0917+458 Maltby *et al.* (1963) comment that the identification may be linked to a nearby galaxy by a faint bridge of optical emission.
1040+317 The galaxy appears multiple; optical position is that of the central nucleus.
1113+295 Peterson (1970) gives a red shift of 0.029 for the cluster Abell 1213. The identification (z = 0.0489) is probably not assoicated with the cluster if both red shifts are correct.
1140+217 Previously identified incorrectly with VV4-28-33 (Aizu 1966). The new identification appears asymmetric or possibly double on the *Sky Atlas*, and appears brighter on the blue print by $\sim 0^m.5$.
1151+295 Olsen's (1970) finding chart depicts a group of three galaxies, of which the proposed identification is the most Northerly.
1350+316 The galaxy is highly flattened and has a peculiar morphology. Sandage (1966) suggests that it may be an incipient spiral. The extent of the low-level radio emission away from the optical image would be unusual for a spiral galaxy.
1446+206 The identification proposed by Hazard *et al.* (1970) is 20 arcsec South of that proposed here, and lies well outside the radio structure. Our identification is that of Olsen (1970).
1452+166 The optical position is that of the slightly blue image near the small-diameter radio component. The red shift is estimated on the assumption that this object is a galaxy; the image is too faint to be classifiable with confidence.
1511+263 The optical position is that of the Northern nucleus of the double galaxy; the other nucleus is ~7 arcsec South.
2335+267 The optical position is that of the brighter nucleus of the double system.

References in Table IV

Position References

1. Goodson *et al.* 1978
2. Fanti *et al.* 1976
3. Griffin 1963
4. Wills *et al.* 1973
5. Véron 1966
6. Riley and Pooley 1975

Redshift References

7. Sargent 1973a
8. Colla *et al.* 1975b
9. Humason *et al.* 1956
10. Burbidge and Strittmatter 1972
11. Sargent 1973b
12. Tritton 1972
13. Matthews *et al.* 1964
14. Adams and Rudnick 1977
15. Wills 1967
16. Moffet 1972
17. Burbidge 1970
18. Schmidt 1965
19. Sandage 1967
20. Sandage 1966
21. Minkowski 1961

Finding Charts

22. Merkelijn *et al.* 1968
23. Colla *et al.* 1975b
24. Wyndham 1966
25. Windram and Kenderdine 1969
26. Olsen 1970
27. Griffin 1963
28. Adams and Rudnick 1977
29. Merkelijn 1968
30. Willson 1972
31. Wills *et al.* 1973
32. Maltby *et al.* 1963
33. This paper, Plate I
34. Grueff and Vigotti 1972
35. Kuhr 1977
36. Hazard *et al.* 1970
37. Westerlund and Wall 1969
38. Wyndham 1965

tended-source area randomly, and only for 0109+492 is the probability >5%.

The radio bridges ("jets") in 0055+300 and 0844+319 place these identifications beyond doubt (first criterion), and in 1557+708 and 2229+391 the optical identifications are so bright ($m_V \sim 12^m.5$) that the probability of the galaxy lying by chance in the search area (second criterion) is <0.1%. The remaining marginal identifications of class T and C sources, 0109+492 and 1502+262, are both weakly supported by the radio morphology (first criterion): The small components lie near the radio centroids and the major axes of elongation. If the search areas were restricted on the evidence of the actual radio morphology, and if the probability of occurrence of the radio source in the galaxy were assessed using the radio luminosity function for elliptical galaxies

© American Astronomical Society • Provided by the NASA Astrophysics Data System

1978AJ.....83..704B

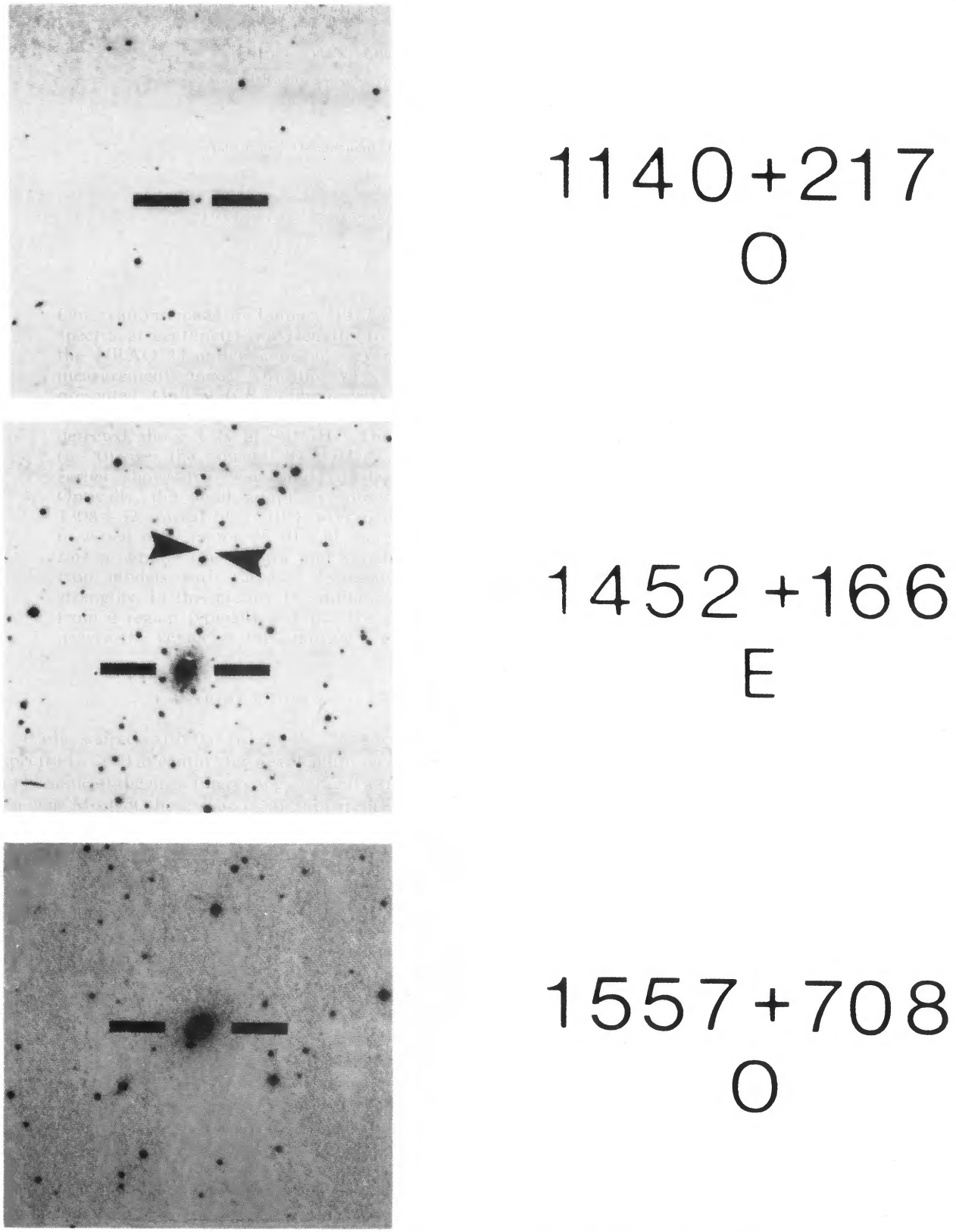

FIG. 6. Finding charts for three radio sources, reproduced from the National Geographic Society—Palomar Observatory Sky Atlas, courtesy of Hale Observatories. Letter codes denote color sensitivity of print (E − red; O − blue). 1452+166: straight bars mark Schilizzi's (1975) identification; arrowheads mark object coincident with small-diameter radio source.

© American Astronomical Society • Provided by the NASA Astrophysics Data System

1978AJ.....83..704B

© American Astronomical Society • Provided by the NASA Astrophysics Data System

1978AJ.....83..704B

derived by Auriemma *et al.* (1977), both identifications would be acceptable at the 99% confidence level.

The three identifications of class L structures can be appraised only on the probability that the optical candidate lies in the radio area by chance, as in these sources the optical identification does not lie at the position of the small-diameter radio component. The probability of misidentification with a field elliptical is ~1% for 1151+295, ~5% for 1420+198 and ~0.5% for 1446+206.

The two sources classified L(H) in Table III each have optical counterparts within one arcsec of the small component and are secure identifications at the 99% confidence level despite the fact that the optical objects are not particularly close to the source centroids. As discussed in Sec. III*d*, these sources may be asymmetric doubles or perhaps head–tails.

The identification of 1452+166 (Fig. 4f) is enigmatic. The *a priori* probability that the small 200-mJy component lies so close to the extended structure is only 0.8%. This component coincides with an $18^{m}.3$ slightly blue image; if this is the identification then the overall morphology would be a wide-angle tail such as those found in some Abell clusters by Rudnick and Owen (1977). There is, however, a 15^{m} galaxy near the radio centroid (Schilizzi 1975) which is the identification favoured by our second criterion. As there is no detectable emission >10 mJy from this 15^{m} galaxy at either 2.7 or 8.1 GHz, the identification must be considered ambiguous until a more detailed radio map permits application of the first (morphological) criterion.

c) Absolute Magnitudes of the Identifications

Thirty-seven of our proposed identifications have measured redshifts. We have assigned redshifts to the other eleven by estimating their apparent magnitudes. B. Guindon and the authors estimated the apparent visual magnitudes of all 48 galaxies containing small-diameter radio components by comparing their images on the red and blue *Palomar Sky Atlas* prints with those of galaxies in the central region of the Coma Cluster for which photovisual magnitudes have been given by Rood (1969). The magnitude estimates were corrected for average galactic extinction adopting the law $\Delta m = 0.25$ $(\csc|b| - 1)$ and are thought to be accurate to about $0^{m}.5$.

After applying the visual K-corrections for giant elliptical galaxies given by Oke and Sandage (1968), the mean absolute magnitude of the thirty-four systems with measured redshifts and coincident small-diameter radio components was $\langle M_V \rangle = -23^{m}.17 \pm 0^{m}.12$ (taking H_0 = 50 km sec^{-1} Mpc^{-1}). We note that this is close to the value of $\langle M_V \rangle = -22^{m}.99$ given for radio galaxies by Sandage (1972). Assuming that the eleven systems without measured redshifts have the same mean m_V-z relation, we can assign redshifts on the basis of our estimated magnitudes with an expected standard error of ~35% (corresponding to our observed standard deviation in M_V of $0^{m}.7$).

Table IV summarizes the results of the optical identification study. Column 1 gives the source name (IAU convention). Column 2 identifies the brighter galaxies by their numbers in the NGC or Vorontsov–Velyaminov catalogs. The optical positions of the centers of the galaxies are listed with their errors in Columns 3 and 4. Columns 5 and 6 give the offsets in arc seconds between the optical and small-diameter radio positions (DRA = optical R.A. minus radio R.A., DDEC = optical declination minus radio declination). Only for the three definite class L structures as either offset significantly greater than 1.5 arcsec. Column 7 gives our estimate of m_V for the galaxy, including the galactic extinction correction. Column 8 lists measured redshifts (no parentheses) and redshifts estimated from our apparent magnitudes as described above (parentheses). Column 9 codifies references for the optical positions, redshifts and identification finding charts (see footnotes to the Table). New finding charts are given for three sources in Fig. 6.

V. THE NATURE OF THE SMALL-DIAMETER COMPONENTS

a) Classification and Radio Parameters

If the component coincides with the identification we term it a radio "core." If the component does not coincide with the identification, we term it "lobe fine structure." For most of the sources discussed here, our use of the term "radio core" is identical to that of Colla *et al.* (1975a), except that their categorization is based on data of lower angular resolution than ours. Our terminology is also similar to that discussed by Jenkins and McEllin (1977); in particular our term "lobe fine structure" refers to the features they describe as "hot spots." Presence of what we describe as lobe fine structure as also the principal characteristic of the class II morphology of Fanaroff and Riley (1974).

Table V gives physical parameters of the small-diameter components. Column 1 gives the source designation and Column 2 the classification of the component as core or lobe (lobe fine structure). The 2.7-GHz monochromatic luminosity of the small component is given in Column 3; that of the entire source in Column 4. Column 5 gives the percentage of the total monochromatic luminosity which is contributed by the small component (Column 3 divided by Column 4) and Column 6 the spectral index α of the small component between 2.7 and 8.1 GHz, on the convention $S(\nu) \propto \nu^{-\alpha}$. In Column 7 are the absolute visual magnitudes of the optical identifications for which redshifts have been measured directly. Column 8 gives the largest angular size using the diameter distance implied by the redshift from Table IV). H_0 = 50 km sec^{-1} Mpc^{-1} and 8q = 0.5 have been assumed throughout.

The range of small-component luminosities is from

© American Astronomical Society • Provided by the NASA Astrophysics Data System

1978AJ.....83..704B

TABLE V. Physical parameters of small components.

Source name	Component type	$\log_{10}P_{2.7}$ (Component)	$\log_{10}P_{2.7}$ (Source)	% Flux	Spectral index	M_V	Overall size (kpc)
0043+201	CORE	23.96	25.20	5.8	0.05	−23.5	327
0055+300	CORE	23.79	24.26	33.8	−0.15	−23.5	1429
0104+321	CORE	22.95	24.64	2.1	−0.40	−23.4	172
0109+492	CORE	23.65	25.39	1.8	>0.09	−23.5	947
0158+293	CORE	24.31	25.86	<2.8	<0.46	−24.0	186
0206+355	CORE	23.75	24.93	6.5	−0.21	−23.3	51
0220+427	CORE	23.66	25.02	4.3	0.32	−23.1	211
0309+390	CORE	24.78	26.12	<4.5	<0.32	−24.4	205
0331+391	CORE	23.67	24.14	34.0	0.20	−23.1	15
0349+212	CORE	24.34	25.46	7.5	0.27	−23.3	164
0623+264	CORE?	24.95	25.77	15.1	−0.11		41
0642+215	CORE	25.89	26.42	29.4	0.22		181
0652+426	CORE	24.41	24.90	32.9	0.20		69
0712+534	CORE	23.50	24.74	5.9	0.42		35
0714+286	CORE	23.91	25.24	<4.6	<−0.03	−23.1	105
0755+379	CORE	24.16	25.16	10.1	−0.07	−24.0	175
0844+319	CORE	23.86	25.15	5.1	0.20	−24.2	542
0917+458	CORE	24.72	26.80	0.8	−0.07	−23.4	688
1003+351	CORE	25.97	26.19	59.8	0.81	−23.0	5843
1040+317	CORE	23.47	24.45	10.4	0.22	−21.9	30
1113+295	CORE	23.52	25.14	2.4	−0.23	−22.9	105
1123+203	CORE?	25.30	25.66	43.6	0.14	−23.7	246
1140+217	CORE	24.39	25.45	8.8	0.56		76
1142+198	CORE	23.68	24.74	8.6	0.15	−21.9	58
1151+295	LOBE	25.45	26.67	6.0	−0.07	−23.2	116
1316+299	CORE	23.77	25.26	3.2	−0.10	−22.7	178
1322+366	CORE	22.91	23.92	9.7	−0.10	−22.0	23
1346+268	CORE	24.18	24.91	18.5	0.66	−23.5	20
1350+316	CORE	25.34	25.42	82.8	0.77	−23.2	122
1420+198	LOBE	26.38	26.90	29.6	1.02		485
1446+206	LOBE	25.97	26.21	57.7	1.11	−22.4	74
1452+166	?	25.72	26.40	20.8	0.04		1112
1502+262	CORE	24.06	25.61	2.8	0.47	−21.6	719
1511+263	CORE	25.03	26.09	8.7	0.91	−23.0	343
1553+245	CORE	23.65	24.11	35.0	0.26	−22.3	23
1557+708	CORE	22.69	24.23	2.9	−0.54		208
1626+396	CORE	23.83	24.72	12.9	0.31	−24.1	75
1658+302	CORE	23.78	24.56	16.4	−0.02		141
1744+557	CORE	23.95	24.41	35.2	−0.01	−23.2	223
1759+211	CORE	23.93	25.08	7.1	0.46		179
1833+326	CORE	24.51	25.73	6.1	0.19	−23.9	416
1834+196	CORE	23.34	24.12	16.5	0.15	−22.1	211
1842+455	CORE	24.32	26.08	1.7	0.29	−24.0	91
1845+797	CORE	24.79	25.97	6.6	−0.30	−22.2	345
1940+504	CORE	23.06	24.55	3.2	0.57	−22.6	39
2229+391	CORE	22.73	24.53	1.6	−0.09	−22.5	168
2234+386	CORE	23.91	25.15	5.9	0.41		183
2335+267	CORE	24.04	25.22	6.6	0.15	−23.3	266

$\sim 8 \times 10^{22}$ to $\sim 2 \times 10^{26}$ W Hz^{-1} at 2.7 GHz, the upper limit surpassing the total luminosities of most sources in the program. Many of the small components, if seen in isolation, would not be especially underluminous in comparison with the general radio-galaxy population. Most of the small components have flat or opaque radio spectra with spectral indices <0.4, but a significant minority has indices >0.4. *We believe this division according to spectral index may reflect a physical distinction between two different classes of object among the radio cores.*

b) *The Compact Cores*

The cores with spectral indices <0.4 are generally unresolved, and the limits on their linear sizes are generally less than 1 kpc. We therefore propose to call these the "compact" cores. Their median 2.7-GHz luminosity is 7×10^{23} W Hz^{-1} and the median absolute magnitude of the galaxies containing them is $\langle M_V \rangle = -23^{m}.2$. There is no evidence that either the total luminosity or the overall size of the extended structure depends on either the fraction of the total luminosity which is contributed by the compact core, or on the spectral index of the compact core. Observational selection against cores with small fractions of the total luminosity forces the *appearance* of correlation (see Fig. 7) between core luminosity and overall luminosity, but we see no sign within this apparent correlation of any possibly real interaction between core and extended-component luminosities. The *fractional* luminosity of the cores does not vary with the overall luminosity over three orders of magnitude in the latter.

Our size limits for the compact cores (and the *VLBI*

© American Astronomical Society • Provided by the NASA Astrophysics Data System

1978AJ.....83..704B

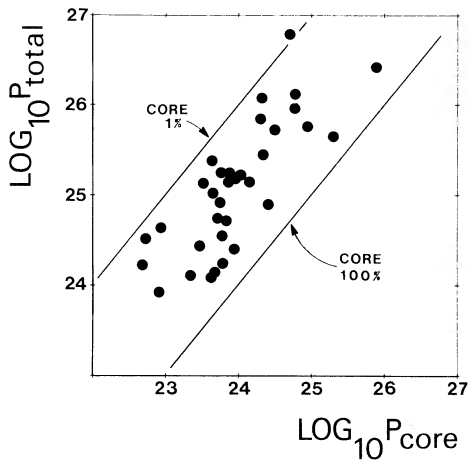

FIG. 7. Logarithimic plot of the 2.7-GHz luminosity of entire source (W Hz^{-1}) against the luminosity of the compact core component, if any. The lines show the accessible boundaries of the plot defined by a) the detection requirement that the core contain at least 1% of the total flux density and b) the limit in which it would contain 100% of the emission. There is no sign of a correlation between compact core luminosity and total luminosity within these limits.

observations of some of them) suggest that they are associated with small-scale ($\leq$ 100 pc) activity in galactic nuclei.

c) *The Extended Cores*

In contrast to the cores with spectral indices <0.4, several cores with indices >0.4 are definitely resolved and have linear sizes in the range 2–6 kpc. Such dimensions are larger than those normally envisioned for the highly condensed regions of galactic nuclei, and we conjecture that the extended cores may be more intimately related to the processes of energy transport and collimation in the large-scale structures than are the compact cores. Although our present sample contains only ten extended cores, two trends are evident which support this conjecture.

First, the extended cores show evidence of conforming to a spectrum-luminosity relation analogous to that found for straight-spectrum radio galaxies (Bridle *et al.* 1972a, Véron *et al.* 1972, MacLeod and Doherty 1972) but with a more rapid increase of the spectral index with luminosity. Figure 8 plots the spectral indices of the extended cores against their 2.7-GHz luminosities; also shown is the mean spectral index—luminosity relation from Bridle *et al.* (1972a), scaled to 2.7 GHz. The correlation coefficient between spectral index and the logarithm of the luminosity for the extended cores is 0.87. The correlation is statistically significant and suggests that the (unknown) mechanism underlying the spectrum-luminosity relation operates in the extended cores as well as in the larger-scale emission.

Second, the two examples of lobe fine structure with high spectral indices appear to conform to the same relation as do the extended cores (see open circles in Fig. 8), suggesting continuity of physical conditions between the extended cores and the structures of comparable linear scale in the outer lobes.

We do not find that the linear sizes or luminosites of the extended structures depend significantly on the measured properites of the extended cores. Tests for interaction between these cores and the overall source luminosities are, of course, biased on the selection effect illustrated in Fig. 7 and are restricted in significance by the small number of extended cores presently known.

However the trends in the parameters of the extended cores are interpreted, the extended cores appear more systematic in their measurable properties than do the compact cores. This may be due to self-absorption phenomena in compact cores with very small linear scales, high energy densities and magnetic field strengths. It is possible that the extended cores detected here contain weak compact cores which cannot yet be distinguished from them; observations of the extended cores at both arcsec and milliarcsec resolution will be necessary to clarify the relation between compact and extended cores and between extended cores and the source-collimating mechanism in radio galaxies.

d) *Absolute Magnitudes versus Core Radio Luminosities*

Table VI shows the mean absolute magnitude for four groups of core sources separated by their 2.7-GHz luminosities. Above a core luminosity of $\sim 10^{23.5}$ W Hz^{-1} the mean optical luminosity is essentially constant. Selection effects force an increase in the mean redshift with

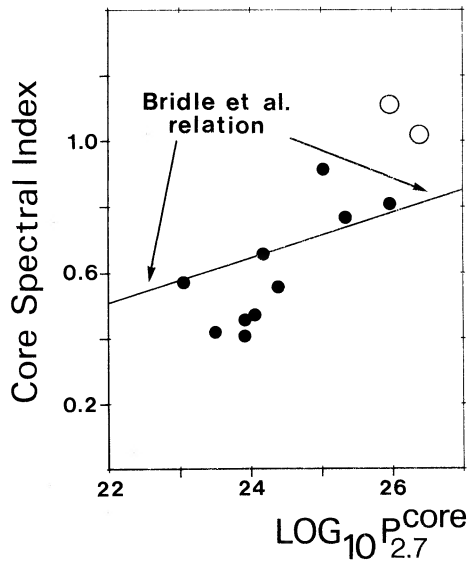

FIG. 8. Spectrum-luminosity correlation for extended cores (●) and lobe fine structure (○). The spectral index is the two-point spectral index between 2.7 and 8.1 GHz for the small component. The luminosity is the monochromatic luminosity at 2.7 GHz in W Hz^{-1}.

© American Astronomical Society • Provided by the NASA Astrophysics Data System

1978AJ.....83..704B

TABLE VI. Mean absolute visual magnitudes for radio cores separated by 2.7-GHz luminosity.

2.7-GHz luminosity group (WHz^{-1})	$\langle M_V \rangle$	σ_M	$\langle z \rangle$	Number of sources
$P < 10^{23.5}$	$-22^m42 \pm 0^m25$	0.56	0.022 ± 0.003	6
$10^{23.5} < P < 10^{24}$	-23.17 ± 0.17	0.62	0.047 ± 0.008	14
$10^{24} < P < 10^{24.5}$	-23.36 ± 0.34	0.84	0.080 ± 0.019	7
$P > 10^{24.5}$	-23.35 ± 0.23	0.66	0.104 ± 0.018	8

core luminosity throughout the four groups (Table VI). The low mean optical luminosity below $10^{23.5}$ W Hz^{-1} at 2.7 GHz may therefore be due to the smallness of the volume sampled in that group, coupled with the rarity of elliptical galaxies brighter than $M_V = -23^m$.

Our results for these 35 cores are consistent with the lack of correlation between the optical and 5-GHz core luminosities of the 16 3CR elliptical galaxies with central components reported by Longair (1975). Longair did not differentiate between compact and extended cores; in our sample the two types of core are similarly distributed in the optical-radio luminosity plane so we have combined them in Table VI.

e) Fractional Core Luminosity and Source Morphology

Rowan-Robinson (1977) has suggested that the fractional luminosity of the core may be correlated with the morphology of the extended emission. No such correlation is present in our data based on the radio classes given in Table III. The 25 sources classified as T, the 9 classified T(C) or C(T) and the 6 classified C have median fractional luminosites of 5.9%, 6.6%, and ~7.6%, respectively. It should be recalled however that our sample favors optically bright galaxies, so that a correlation depending mainly on galaxies of high radio luminosity might not appear in our data.

f) The Small Component in 1151+295

This component is a striking example of a luminous, flat-spectrum unresolved feature in an end-of-lobe location. There is no candidate for a separate identification of this <0.2 arcsec feature on the *Palomar Sky Atlas* prints. The 19^m4 galaxy we have identified with the radio structure lies near a poorly-defined radio feature which could be a weak extended core. It is unlikely that the source is misidentified or that it is a distant head-tail system whose identification lies below the print limit. The fact that the small component is unresolved on our 35-km baselines implies a linear size less than 1.1 kpc; this is not particularly small (for lobe fine structure) because the optical identification ($z = 0.3292$) is the most remote in our present sample.

The significance of 1151+295 for identification work is that it illustrates that detection of a sub-second-of-arc flat-spectrum radio component need not lead directly to the optical identification of an extended source.

VI. ALTERNATIVE IDENTIFICATION CRITERIA

a) The Radio Centroid

Extended sources with no detectable small-diameter components must be optically identified without the aid of radio core emission; the identifications must therefore rely on weaker criteria than the close optical-radio position coincidences used here. The radio centroid has often been used as an identification indicator because it is readily measured at low resolution. There is little astrophysical basis for its use, however, and the existence of head–tail structures ensures that radio centroids, even if they were unique as the frequency varied, *cannot* locate all correct identifications. Our data give knew empirical support to the practise of using the radio centroids as guides to identifying basically bifurcated structures (as opposed to head–tail systems).

We have determined the position offsets between the 2.7-GHz centroids and the optical identifications made in Sec. IV on the basis of radio core positions. For most sources, the 2.7-GHz centroid can be found with an accuracy of a few seconds of arc using our maps or those from the literature. For a few sources the mapped flux density was significantly less than the total detected by our pencil-beam observations; the centroid was then determined from the pencil-beam data. Figure 9 shows

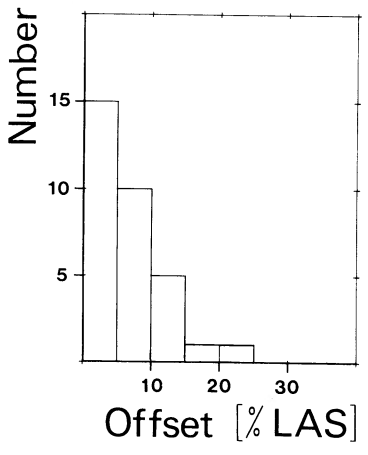

FIG. 9. Frequently histogram of angular offsets between core components and 2.7-GHz centroids of bifurcated structures, expressed as percentages of the source LAS (Section Va). Over 90% of the cores lie within 0.15(LAS) of the 2.7-GHz centroid.

© American Astronomical Society • Provided by the NASA Astrophysics Data System

1978AJ.....83..704B

the histogram of the position offsets (right ascension and declination combined) between our optical positions and the 2.7-GHz centroids, normalized in each case to the largest angular size (LAS) of the extended structure. Over 90% of the optical identifications lie within 0.15 (LAS) of the radio centroids.

Guindon (1976) compared the linear sizes, luminosites and symmetry parameters of well-identified triple and double sources (i.e., doubles with and without radio cores) and showed that the physical characteristics of the extended emission do not significantly depend on whether or not a radio core is detectable. This being so, it is reasonable to assume that the locations of the true identifications of extended double sources without radio cores will follow the general pattern evidenced in Fig. 9, i.e., that ~90% of the true identifications of bifurcated sources will be found within 0.15 (LAS) of the radio centroids.

b) The Brightest Galaxy

In three sources—0642+214, 1452+166 and 1511+263—an identification based on a radio core is not the brightest galaxy in the area covered by the radio structure. In 0642+214 a galaxy $0^m.5$ brighter than the identification lies significantly South of the 2.7-GHz centroid, near the peak brightness in the Southern radio lobe (see Fig. 2d). 1452+166 was discussed in Sec. IV *b* above; the radio core may be a background source unrelated to the extended emission while a galaxy nearly 3^m brighter than the core object lies near the 2.7-GHz centroid.

The core of 1511+263 coincides with the more northerly of two galaxies ~7 arcsec apart; the system was described by Matthews *et al.* (1964) as having a common envelope and is usually classified as a dumb-bell galaxy. The nucleus/galaxy containing the radio core is the fainter by about $0^m.4$ on the *E* (red) *Sky Atlas* print but appears as bright as the Southern nucleus/galaxy on the *O* (blue) print. Thus the active radio nucleus/galaxy is relatively bluer, which might indicate a greater non-thermal contribution to its optical emission.

The probabilistic statement that the brightest galaxy is the least likely to be in the search area by chance therefore combines with physical association between radio cores and luminous galaxies to make brightest-galaxy identifications generally reliable when the *a priori* probability of a chance superposition is low. Identifications with bright galaxies within 0.15(LAS) of the radio centroids of double sources should have particularly high probabilities of being correct if double structures without presently-detectable cores are indeed generically related to the systems discussed here.

VI. CONCLUSIONS

The principal results of this paper can be summarized as follows:

(a) Combination of precise radio positions for small-diameter components in 48 extended sources and precise optical positions for the centers of galaxies has led to essentially unambiguous optical identifications for 44 extended structures.

(b) *The small radio components which coincide with the galaxy centers* (radio cores) *are probably of two kinds* distinguishable primarily by their radio spectra—*compact cores* with spectral indices <0.4 and *extended cores* with indices >0.4. The compact cores are generally less than 1 kpc in linear diameter (and many are significantly smaller than this) whereas the extended cores are often several kpc in size. In our sample the extended cores comprise ~20% of all cores.

(c) *The spectra and luminosities of the compact cores do not correlate significantly with the luminosities or sizes of the extended emission.* Selection effects produce the *appearance* of correlation between compact core luminosity and the total luminosity, but there is no evidence for any real interaction between these quantities over more than three decades in luminosity.

(d) *The extended cores display a spectrum luminosity relation* in which the spectral index increases more rapidly with luminosity than in the total emission of straight-spectrum radio galaxies.

(e) In all sources but 1452+166 and 1511+263, *brightest galaxy identifications closer than 0.15(LAS) to the radio centroid would be identical to our radio core identifications for sources with clearly bifurcated overall structures.* Extended double sources can apparently be identified with the brightest galaxy near their radio centroid with greater reliability than we might expect from the present state of theoretical models of the radio-galaxy phenomenon.

(f) The sources 1151+295 and 1452+166 demonstrate that small-diameter components with flat radio spectra do not always coincide with the optical identification or with the brightest galaxy in the field, so that searches for compact radio components cannot resolve all of the uncertainties inherent in the identification process for extended sources.

Dr. G. W. Brandie and Dr. B. Guindon contributed extensively to the initial inspections of the Sky Atlas which defined the sample of elliptical galaxies to be studied in this series of papers, and also took part in the observing and early data reductions at NRAO. We particularly thank Dr. Guindon for his comprehensive documentation of the optical fields near the program sources, which expedited the optical identification work reported here, and Dr. Brandie for careful criticism of an earlier version of this paper.

This research was partly supported by grants to AHB from the National Research Council of Canada and from Queen's University. The National Radio Astronomy Observatory is operated by Associated Universities, Inc., under contract with the National Science Foundation.

© American Astronomical Society • Provided by the NASA Astrophysics Data System

1978AJ.....83..704B

REFERENCES

Adams, M. T., and Rudnick, L. (1977). Astron. J. **82,** 857.
Aizu, K. (1966). Publ. Astron. Soc. Jpn. **18,** 219.
Allen, C. W. (1973). *Astrophysical Quantities* 3rd Edition, (Athlone, London) p. 289.
Auriemma, C., Perola, G. C., Ekers, R., Fanti, R., Lari, C., Jaffe, W. J., and Ulrich, M.-H. (1977). Astron. Astrophys. **57,** 41.
Branson, N. J. B. A., Elsmore, B., Pooley, G. G., and Ryle, M. (1972). Mon. Not. R. Astron. Soc., **156,** 377.
Bridle, A. H. and Brandie, G. W. (1973). Astrophys. Lett. **15,** 21.
Bridle, A. H. and Goodson, R. E. (1977). J. R. Astron. Soc. Can. **71,** 240.
Bridle, A. H., Davis, M. M., Fomalont, E. B., and Lequeux, J. (1972b). Astron. J., **77,** 405.
Bridle, A. H., Davis, M. M., Meloy, D. A., Fomalont, E. B., Strom, R. G. and Willis, A. G. (1976). Nature, **262,** 179.
Bridle, A. H., Kesteven, M. J. L., and Brandie, G. W. (1977). Astron. J., **82,** 21.
Bridle, A. H., Kesteven, M. J. L., and Guindon, B. (1972a). Astrophys. Lett. **11,** 27.
Burbidge, E. M. (1970). Astrophys. J. Lett. **160,** L33.
Burbidge, E. M., and Strittmatter, P. (1972). Astrophys. J. Lett., **172,** L37.
Caswell, J. L., and Wills, D. (1967). Mon. Not. R. Astro. Soc. **145,** 181.
Colla, G., Fanti, C., Fanti, R., Gioia, G., Lari, C., Lequeux, J., and Ulrich, M.-H. (1975a) Astron. Astrophys. **38,** 209.
Colla, G., Fanti, C., Fanti, R., Gioia, I., Lari, C., Lequeux, J., Lucas, R., and Ulrich, M.-H. (1975b). Astron. Astrophys. Suppl. **20,** 1.
Fanaroff, B. L., and Riley, J. M. (1974). Mon. Not. R. Astron. Soc. **167,** 31P.
Fanti, C., Fanti, R., Gioia, I., Lari, C., Parma, P., and Ulrich, M.-H. (1977). Astron. Astrophys. Suppl **29,** 279.
Fanti, R., Lari, C., Spencer, R. E., and Warwick, R. S. (1976). Mon. Not. R. Astron. Soc. **174,** 5P.
Fomalont, E. B., and Bridle, A. H. (1978). Astron. J. **83,** 724.
Fomalont, E. B., and Miley, G. K. (1975). Nature, **257,** 99.
Fomalont, E. B., Bridle, A. H., and Davis, M. M. (1974). Astron. Astrophys. **36,** 273.
Goodson, R. E., Palimaka, J. J., and Bridle, A. H. (1978). To be submitted to Astron. J. (Paper III).
Griffin, R. F. (1963). Astron. J. **68,** 421.
Grueff, G., and Vigotti, M. (1972). Astron. Astrophys. Suppl. **6,** 1.
Guindon, B. (1976). Ph.D. thesis, Queen's University at Kingston.
Harris, A. (1972). Mon. Not. R. Astron. Soc. **158,** 1.
Hazard, C., Jauncey, D. L., and Backer, D. C. (1970). Astron. J., **75,** 1039.
Högbom, J. A. (1974). Astron. Astrophys. Suppl. **15,** 417.
Högbom, J. A. and Carlsson, I. (1974). Astron. Astrophys. **34,** 341.
Humason, M. L., Mayall, N. U., and Sandage, A. R. (1956). Astron. J. **51,** 97.
Jaffe, W., and Perola, G. C. (1974). Astron. Astrophys. **31,** 223.
Jenkins, C. J., and McEllin, M. (1977). Mon. Not. R. Astron. Soc. **180,** 219.
Jenkins, C. J., Pooley, G. G., and Riley, J. M. (1977). Mem. R. Astron. Soc. **84,** 61.
Kesteven, M. J. L., Bridle, A. H., and Brandie, G. W. (1976). Astron. J. **81,** 919.
Kuhr, H. (1977). Astron. Astrophys. Suppl. **29,** 139.
Longair, M. S. (1975). Mon. Not. R. Astron. Soc. **173,** 309.
Macdonald, G. H., Kenderdine, S., and Neville, A. C. (1968). Mon. Not. R. Astron. Soc., **138,** 259.
Mackay, C. D. (1969). Mon. Not. R. Astron. Soc. **145,** 31.
Mackay, C. D. (1971). Mon. Not. R. Astron. Soc. **151,** 421.
MacLeod, J. M., and Doherty, L. H. (1972). Nature, **238,** 88.
Maltby, P., Matthews, T. A., and Moffet, A. T. (1963). Astrophys. J. **137,** 153.
Matthews, T. A., Morgan, W. W., and Schmidt, M. (1964). Astrophys. J. **140,** 35.
Merkelijn, J. K. (1968). Aust. J. Phys. **21,** 903.
Merkelijn, J. K., Simmins, A. J., and Bolton, J. G. (1968). Aust. J. Phys. **21,** 523.
Miley, G. K., and van der Laan, H. (1973). Astron. Astrophys. **28,** 359.
Minkowski, R. (1961). Astron. J. **66,** 558.
Moffet, A. T. (1972). *Stars and Stellar Systems,* Vol. 9, Ch. 7, edited by Sandage, A., Sandage, M., and Kristian, J., (Univ. Chicago P., Chicago).
Northover, K. J. E. (1973). Mon. Not. R. Astron. Soc. **165,** 369.
Northover, K. J. E. (1976). Mon. Not. R. Astron. Soc. **177,** 307.
Oke, J. B. and Sandage, A. R. (1968). Astrophys. J. **154,** 21.
Olsen, E. T. (1970). Astron. J. **75,** 764.
Owen, F. N., and Rudnick, L. (1976). Astrophys. J. Letts. **205,** L1.
Owen, F. N., Rudnick, L., and Peterson, B. M. (1977). Astron. J. **82,** 677.
Peterson, B. (1970). Astron. J. **75,** 695.
Pooley, G. G., and Henbest, S. N. (1974). Mon. Not. R. Astron. Soc. **169,** 477.
Preuss, E., Pauliny-Toth, I. I. K., Witzel, A., Kellermann, K. I., and Shaffer, D. E. (1977). Astron. Astrophys. **54,** 297.
Riley, J. M. (1975). Mon. Not. R. Astron. Soc. **170,** 53.
Riley, J. M., and Branson, N. J. B. A. (1973). Mon. Not. R. Astron. Soc. **164,** 271.
Riley, J. M. and Pooley, G. G. (1975). Mem. R. Astron. Soc. **80,** 105.
Rood, H. J. (1969). Astrophys. J. **158,** 657.
Rowan-Robinson, M. (1977). Astrophys. J. **213,** 635.
Rudnick, L., and Owen, F. N. (1977). Astron. J. **82,** 1.
Sandage, A. R. (1966). Astrophys. J. **145,** 1.
Sandage, A. R. (1967). Astrophys. J. Lett. **150,** L45.
Sandage, A. R. (1972). Astrophys. J. **178,** 25.
Sargent, W. L. W. (1973a). Publ. Astron. Soc. Pac. **85,** 281.
Sargent, W. L. W. (1973b). Astrophys. J. Lett., **182,** L13.
Schilizzi, R. T. (1975). Mem. R. Astron. Soc. **79,** 75.
Schilizzi, R. T. (1976). Astron. J. **81,** 946.
Schmidt, M. (1965). Astrophys. J. **141,** 1.
Tritton, K. P. (1972). Mon. Not. R. Astron. Soc. **158,** 277.
Turland, B. D. (1975). Mon. Not. R. Astron. Soc. **172,** 181.
van Breugel, W. J. M. and Miley, G. K. (1977). Nature, **265,** 315.
Véron, M. P., Véron, P., and Witzel, A. (1972). Astron. Astrophys. **18,** 82.
Véron, P. (1966). Astrophys. J. **144,** 861.
Westerlund, B. E., and Wall, J. V. (1969). Astron. J. **74,** 335.
Willis, A. G., Strom, R. G., and Wilson, A. S. (1974). Nature, **250,** 625.
Wills, D. (1967). Astrophys. J. Lett. **148,** L57.
Wills, B. J., Wills, D., and Douglas, J. N. (1973). Astron. J. **78,** 521.
Willson, M. A. G. (1972). Mon. Not. R. Astron. Soc. **156,** 7.
Windram, M. D., and Kenderdine, S. (1969). Mon. Not. R. Astron. Soc. **146,** 265.
Wyndham, J. D. (1965). Astron. J. **70,** 384.
Wyndham, J. D. (1966). Astrophys. J. **144,** 549.

© American Astronomical Society • Provided by the NASA Astrophysics Data System

1978AJ.....83..704B

THE ASTRONOMICAL JOURNAL VOLUME 83, NUMBER 7 JULY 1978

EXTENDED RADIO SOURCES AND ELLIPTICAL GALAXIES
II. A SEARCH FOR RADIO CORES USING THE VLA

E. B. FOMALONT
National Radio Astronomy Observatory[a] Socorro, New Mexico 87801

A. H. BRIDLE
Queen's University at Kingston, Ontario, Canada K7L 3N6
Received 21 February 1978

ABSTRACT

Four antennas of the Very Large Array (VLA) have been used at 4.9 GHz to search for small-diameter radio components in extended radio sources whose optical identifications are uncertain. Thirteen of 21 systems studied have small components ($\lesssim 4$ arcsec in extent) with flux densities ≥ 5 mJy. Eleven of these small components are coincident with galaxies and thus confirm or establish the identification of the sources. In three systems previously identified with close pairs of galaxies (or double-nucleus systems), the position of the radio core lies within the nucleus of one of the two galaxies. The probability that a small-diameter radio source will be detected at random within an extended source is also discussed. The large angular size and the high redshift ($z = 0.2107$) of the identification of 0136+397=4C39.04 imply that it is a "giant" radio galaxy ~ 1.5 Mpc in linear extent. A compact component in 1522+546=3C319 coincides within errors with a very faint optical image that is not the usual identification.

I. INTRODUCTION

This paper is the second of a series describing radio and optical measurements of elliptical radio galaxies. In Paper I (Bridle and Fomalont 1978) we described observations made at 2.7 and 8.1 GHz with the NRAO 4-element interferometer which resulted in the detection of compact components within extended radio galaxies, and we discussed the implications of such observations for making reliable optical identifications of such extended systems. In this paper we report further observations made to improve the reliability of the identifications of 21 radio sources by detecting radio cores in the nuclei of their parent galaxies.

II. OBSERVATIONS AND REDUCTIONS

a) Selection of the Program Sources

The 21 sources observed are among those in a sample of several hundred sources (discussed in Paper I) which could not be reliably identified with an optical object on the evidence either of published high-resolution radio maps or of our observations with the 4-element interferometer at Green Bank. In most cases either several optical candidates lay within the radio structure, or the only optical object in or near the structure had a high probability of being a chance projection. Our aim was to resolve such ambiguities by detecting radio "cores" (i.e., small-diameter components coincident with a galaxy, see Paper I) in the true identifications. All 21 sources had already been mapped with reasonable sensitivity and resolution and were known to have (a) a well-defined major axis of elongation, (b) overall angular size $\gtrsim 20$ arcsec, and (c) possible relationship to an elliptical or SO galaxy. Thus, in order to detect radio cores at the mJy level, both high angular resolution (<5 arcsec) and good sensitivity were requirements for these observations.

b) Instrumentation

The Very Large Array (VLA), now being constructed by NRAO in New Mexico, will ultimately comprise 27 antennas, each of 25-m diameter in a Y-configuration providing baselines up to ~ 30 km. In March–May 1977 four elements of the array were fully operational at frequencies near 5 GHz with a maximum baseline of 4.739 km, providing a resolution of ~ 2 arcsec and (with 50 MHz bandwidth) an rms noise of ~ 1 mJy in less than 30 minutes of observing time.

We calibrated the gain and phase fluctuations in the electronics and the atmosphere by observing small-diameter radio sources with well-known flux densities and positions. Each radio source was observed alternately with one particular calibrator, usually less than 15° away, spending 13 min on source and 7 min on its calibrator with 1 min change time. Each source was observed about nine times spread in hour angle as conveniently as possible in order to maximize the (u,v) coverage. Ob-

[a]Operated by Associated Universities, Inc., under contract with the National Science Foundation.

 0004-6256/78/8307-0725$00.90 © 1978 Am. Astron. Soc.

© American Astronomical Society • Provided by the NASA Astrophysics Data System

1978AJ.....83..704B

TABLE I. Calibrator sources.

Calibrator		$S(4.9)$ Jy[a]	RA (1950.0)	DEC	Sources calibrated
0106 + 013	P0106 + 01	4.23	$01^h06^m04^s.518$	+01°19′00″.47	2357 + 004
0134 + 329	3C48	5.35	01 34 49.827	+32 54 20.63	0136 + 397, 0158 + 293
0316 + 413	3C84	45.6	03 16 29.566	+41 19 51.92	0258 + 356
0430 + 052	3C120	6.85	04 30 31.603	+05 14 59.62	0356 + 102
0552 + 398	DA193	5.21	05 52 01.389	+39 48 21.78	0632 + 263
0736 + 017	P0736 + 01	1.90	07 36 42.517	+01 44 00.32	0819 + 061
0742 + 103	D0742 + 10	3.70	07 42 48.466	+10 18 32.67	0714 + 286
0923 + 392	DA267	7.30	09 23 55.314	+39 15 23.58	0915 + 320, 0916 + 342, 0936 + 361, 0938 + 349
1328 + 307	3C286	7.48	13 28 49.655	+30 45 58.65	1301 + 382, 1308 + 277, 1313 + 072, 1319 + 428, 1430 + 251
1641 + 399	3C345	7.05	16 41 17.608	+39 54 10.84	1522 + 546, 1707 + 344, 1726 + 318
2128 − 123	P2128 − 12	1.94	21 28 52.760	−12 20 23.30	2058 − 135

[a] 1 Jy = 1×10^{-26} w m^{-2} Hz^{-1}.

servations at elevations less than 15° were avoided. In Table I we list the parameters of the calibrator sources. The pointing of the antennas and their relative positions were measured using radio calibrators just prior to each run. The pointing accuracy was about 30 arcsec (1/20 half-power beamwidth) and the antenna positions were obtained with an accuracy of 2 mm.

c) *Data Reduction*

The data were accumulated for 10-s periods at the telescope. After editing the 10-s records for anomalous gain and phase behavior or unusual instrumental conditions, the data were vectorially averaged to 3-min samples. The observed visibilities for each source were then corrected by interpolating the long-term gain and phase performance of the array using the observations of the calibrators. The rms gain fluctuations on time scales ~10 min were ~3%; phase fluctuations varied from ~3° on baselines ≲1 km to ~10° for the 4.7-km baseline.

Radio maps were made from the calibrated data by the usual Fourier methods. As some maps contained significant responses to the extended emission from the sources (which confused the search for weak small-diameter components), high-resolution maps were also made using only the baselines >2 km. Further reductions to determine flux densities and positions of possible radio "cores" depended on the nature of the resulting maps.

In some cases the maps were consistent with noise; upper limits to the flux densities of cores anywhere within the region near the extended emission could then be derived directly from the maps. For many sources a small-diameter component dominated the high-resolution (baselines >2 km) map and its position, intensity and angular size could be found by fitting an elliptical Gaussian model to the observed visibility data; the maps were used to guide the initial choice of model parameters. For a number of sources ≲40 arcsec in extent, we mapped the entire structure using a CLEAN algorithm (Högbom 1974) to deconvolve the effects of our unfilled aperture. The core components could generally be recognized on the CLEAN maps, or upper limits could be set to their intensities as before.

III. RESULTS

a) *Positive Detections*

Table II shows the results for the 13 sources in which we detect small-diameter components. Column 1 gives the source designation (IAU convention and common name) and Column 2 the flux density and its standard error. The radio position and its error are tabulated in the upper row of Columns 3 and 4; if a galaxy lies within 2 arcsec of the radio position, the optical position of the galaxy center (generally from Goodson *et al.* 1978—Paper III in this series) is given in the lower row. The eleven entries with both radio and optical positions represent successful detections of radio "cores." Column 5 gives the angular size of the small component.

Column 6 codifies the overall radio morphology of the source and the relationship to this small-diameter component. The letter codes are those defined in Paper I—structures clearly bifurcated along their major axes are coded T (triple) or L (lobe brightening) according to whether the small-diameter component is located towards the center or the edge of the structure. Less clearly bifurcated structures are coded C (core) or H (head) on the same criterion. The galaxy morphology (E-elliptical, db-double-nucleus galaxy or double galaxy) and visual magnitude corrected for galactic absorption are given in Column 7. Column 8 gives references to finding charts for the identifications and maps of the extended radio source components. Individual sources are discussed in Sec. IV.

b) *Upper Limits*

The eight sources in which we did not detect small-diameter components are listed in Table III. The source names and the upper limit to the 6-cm flux density of any small-diameter component in the area covered by the extended source are given in Columns 1 and 2. Column 3 gives the nominal identification and Column 4 notes

© American Astronomical Society • Provided by the NASA Astrophysics Data System

1978AJ.....83..704B

TABLE II. Radio sources with detected small-diameter components.

Source	$S(4.9)$ mJy	RA (1950)	DEC	Diameter	Class	ID, m_v	References
0136 + 397	13 ± 2	$01^h36^m33^s.59 \pm 0^s.02$	$39°41'51''.5 \pm 0''.5$	<2″	T	db?, $18^m.5$	1, 9
4C39.04		33.58 ± 0.03	51.2 ± 0.7				
0158 + 293	16 ± 3	01 58 43.43 ± 0.02	29 19 17.4 ± 0.4	<2	C(T)	db, 16.2	1, 10
4C29.05		43.49 ± 0.04	16.0 ± 0.4				
0356 + 102	9 ± 3	03 56 10.20 ± 0.04	10 17 32.1 ± 0.7	<4	T	E, 15.0	2, 11
3C98		10.21 ± 0.04	31.7 ± 0.4				
0632 + 263	21 ± 4	06 32 29.52 ± 0.02	26 19 06.4 ± 0.2	~3	T	E, 13.0	3, 9
4C26.23		29.60 ± 0.03	06.4 ± 0.4				
0714 + 286	17 ± 2	07 14 48.02 ± 0.03	28 40 35.4 ± 0.3	<2	T	E, 15.6	4, 10
4C28.18		48.03 ± 0.03	35.9 ± 0.4				
0915 + 320	8 ± 1	09 15 58.46 ± 0.05	32 04 20.1 ± 0.7	<2	T	E, 15.0	5, 12
B20915 + 32		58.53 ± 0.03	20.8 ± 0.4				
0936 + 361	18 ± 4	09 36 50.92 ± 0.03	36 07 35.8 ± 0.4	<2	T	E, 17.4	6, 13
3C223		50.87 ± 0.06	35.0 ± 0.5				
1313 + 072	22 ± 3	13 13 45.94 ± 0.01	07 18 35.4 ± 0.2	<2	T	E, 14.8	7, 14
P1313 + 07		45.97 ± 0.02	35.6 ± 0.4				
1319 + 428	6 ± 2	13 19 05.20 ± 0.05	42 50 56.7 ± 0.6	<4	T	E, 15.7	6, 15
3C285		05.22 ± 0.04	55.7 ± 0.3				
1430 + 251	24 ± 4	14 30 28.22 ± 0.05	25 09 25.4 ± 0.7	≲2	?	No ID	1, 9
4C25.46							
1522 + 546	63 ± 5	15 22 47.68 ± 0.05	54 39 11.3 ± 0.5	≲2	?	ID: see text	6, 9
3C319							
2058 − 135	23 ± 4	20 58 59.27 ± 0.12	−13 30 35.8 ± 1.7	<2	T	E, 14.3	8, 16
P2058 − 13		59.38 ± 0.05	38.2 ± 1.0				
2357 + 004	12 ± 2	23 57 25.07 ± 0.03	00 25 23.4 ± 0.6	<4	C	db, 15.3	7, 9
		25.00 ± 0.04	24.5 ± 0.4				

references to suggested optical identifications and published radio maps.

c) *Radio Maps*

Seven radio maps obtained with the NRAO interferometer at 2.7 GHz or with the VLA at 4.9 GHz are shown in Figs. 1 and 2. We have included only those sources for which comparably detailed maps are not already published. Comments on the individual sources are given in Sec. IV.

IV. NOTES ON INDIVIDUAL SOURCES

a) *0136 + 397 = 4C39.04*

This source was first identified with a galaxy by Olsen (1970). Our inspection of the *Palomar Sky Atlas* showed the image marked by Olsen to be double; the positions of both optical features are given in Paper III. The small component detected by the VLA lies within 1.5 arcsec of the brighter South-preceding image. The redshift of 0.2107 for this system has been measured by Sargent (1973) although he does not state whether the redshift applies to both optical features. The optical field on the red print of the *Palomar Sky Atlas* is sketched in Fig. 1a, which also shows a 2.7-GHz map of the extended radio structure with 52 arcsec by 37 arcsec resolution. The data for this map were obtained by us with the NRAO 3-element interferometer as described in Paper I.

The overall linear size of the structure shown in Fig. 1a is ~1.5 Mpc using $H_o = 50$ km s^{-1} Mpc^{-1} and $q_o = 0.5$. This suggests that 0136 + 397 is a "giant" radio

TABLE III. Upper limits to small-diameter components.

Source	$S(4.9)$ mJy	Nominal ID, m_v	References
0258 + 356	<2	ambiguous	1, 17
4C35.06A			
0802 + 243	<5	E, 14.9	6, 18
3C192			
0819 + 061	<1.5	E, 16.6	6, 14
3C198			
0938 + 399	<5	E, 16.0	6, 13
3C223.1			
1301 + 382	<3	ambiguous	5, 9
4C38.35			
1308 + 277	<4	E, 17.4	6, 13
3C284			
1707 + 344	<2	ambiguous	9, 19
4C34.45			
1726 + 318	<3	E, 17.0	6, 13
3C357			

References to Tables II and III

Finding Charts

1. Olsen (1970)
2. Maltby, Matthews, and Moffet (1963)
3. Merkelijn, Shimmins, and Bolton (1968)
4. Willson (1972)
5. Colla *et al.* (1975)
6. Wyndham (1966)
7. Clarke, Bolton, and Shimmins (1966)
8. Schilizzi (1975)

Map of Extended Structure

9. This paper
10. Bridle and Fomalont (1978). Paper I
11. Branson *et al.* (1972)
12. Fomalont and Bridle (1978)
13. Riley and Pooley (1975)
14. Fomalont (1971)
15. Miley and van der Laan (1973)
16. Schilizzi and McAdam (1975)
17. Rudnick and Owen (1977)
18. Högbom and Carlsson (1974)
19. Owen, Rudnick, and Peterson (1977)

© American Astronomical Society • Provided by the NASA Astrophysics Data System

1978AJ.....83..704B

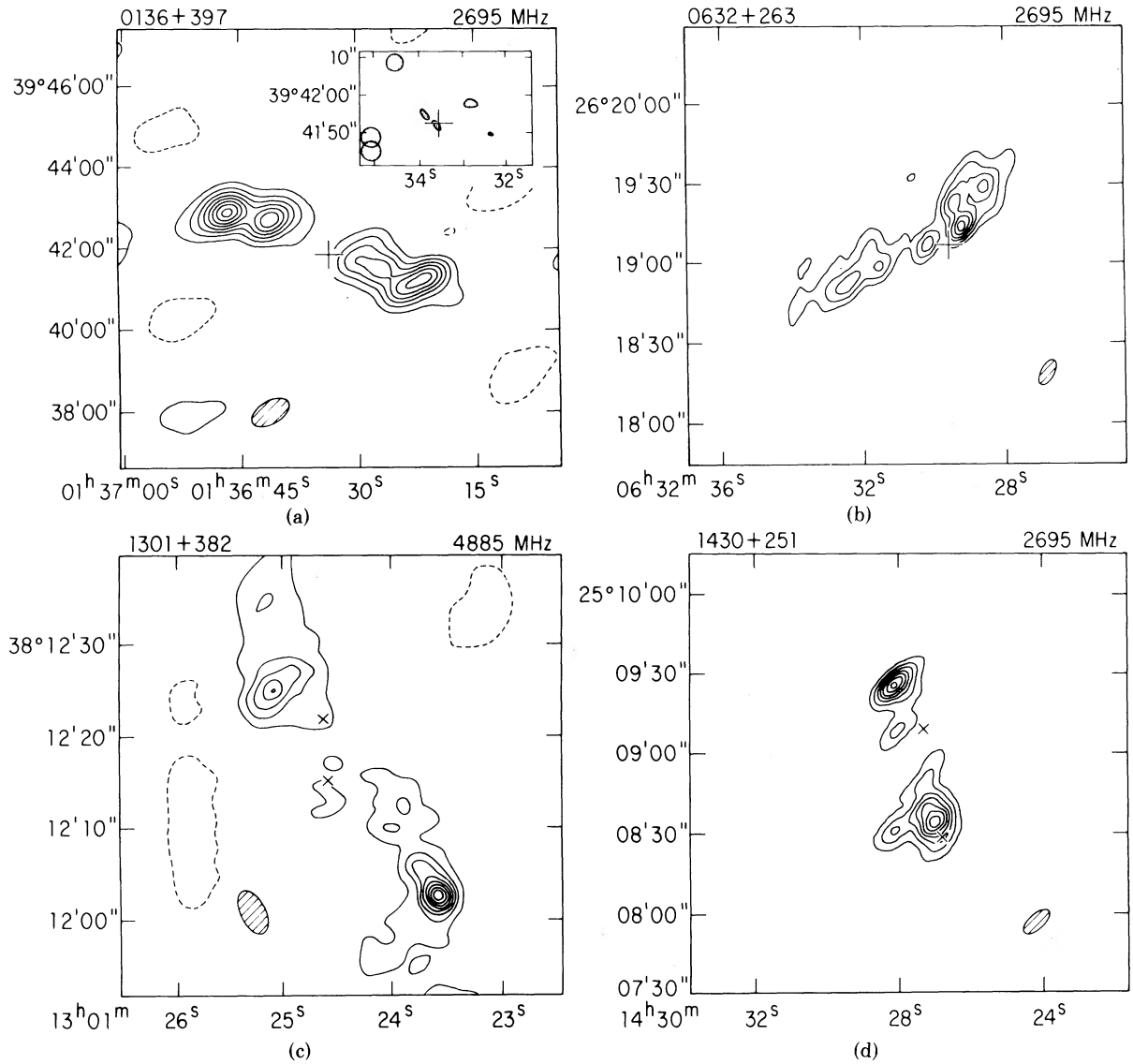

FIG. 1a. 0136 + 397: Each contour level is 9.0 mJy/beam. The location of a 12 mJy small diameter component detected at 4885 mHz is shown by the +. An inset of the optical field around this radio component is shown in the upper right.

FIG. 1b. 0632 + 263: Each contour level is 10.8 mJy/beam. The location of a 17 mJy small-diameter component detected at 4885 MHz, coincident with a $15\overset{m}{.}5$ galaxy, is shown by the +.

FIG. 1c. 1301 + 382: Each contour level is 3.4 mJy/beam. The location of two galaxies in the field are shown by the X's. No small-diameter component was found at 4885 MHz.

FIG. 1d. 1430 + 251: Each contour level is 8.7 mJy/beam. The small-diameter component found at 4885 MHz is the north component in its entirety. Two galaxies in the field are degnated by the *X*'s.

galaxy, similar in linear size to NGC 315 (Bridle *et al.* 1976). The monochromatic power emitted at 2.7 GHz is 1.1×10^{26} W Hz^{-1} making this source the most luminous radio source known with a linear extent greater than 1 Mpc. From the observed spectrum ($S \propto \nu^{-1.0}$) we estimate that the integrated luminosity between 10 MHz and 10 GHz is 2×10^{36} W. By the usual equipartition calculation the minimum energy in radiating particles and magnetic fields is 3×10^{52} joules and the equipartition field is of order 1 to 10 μG depending on the details of the radio structure which are not well- determined.

b) 0158 + 293 = 4C29.05

Olsen (1970) identified this source with a close pair of galaxies. The small-diameter component detected by

© American Astronomical Society • Provided by the NASA Astrophysics Data System

1978AJ.....83..704B

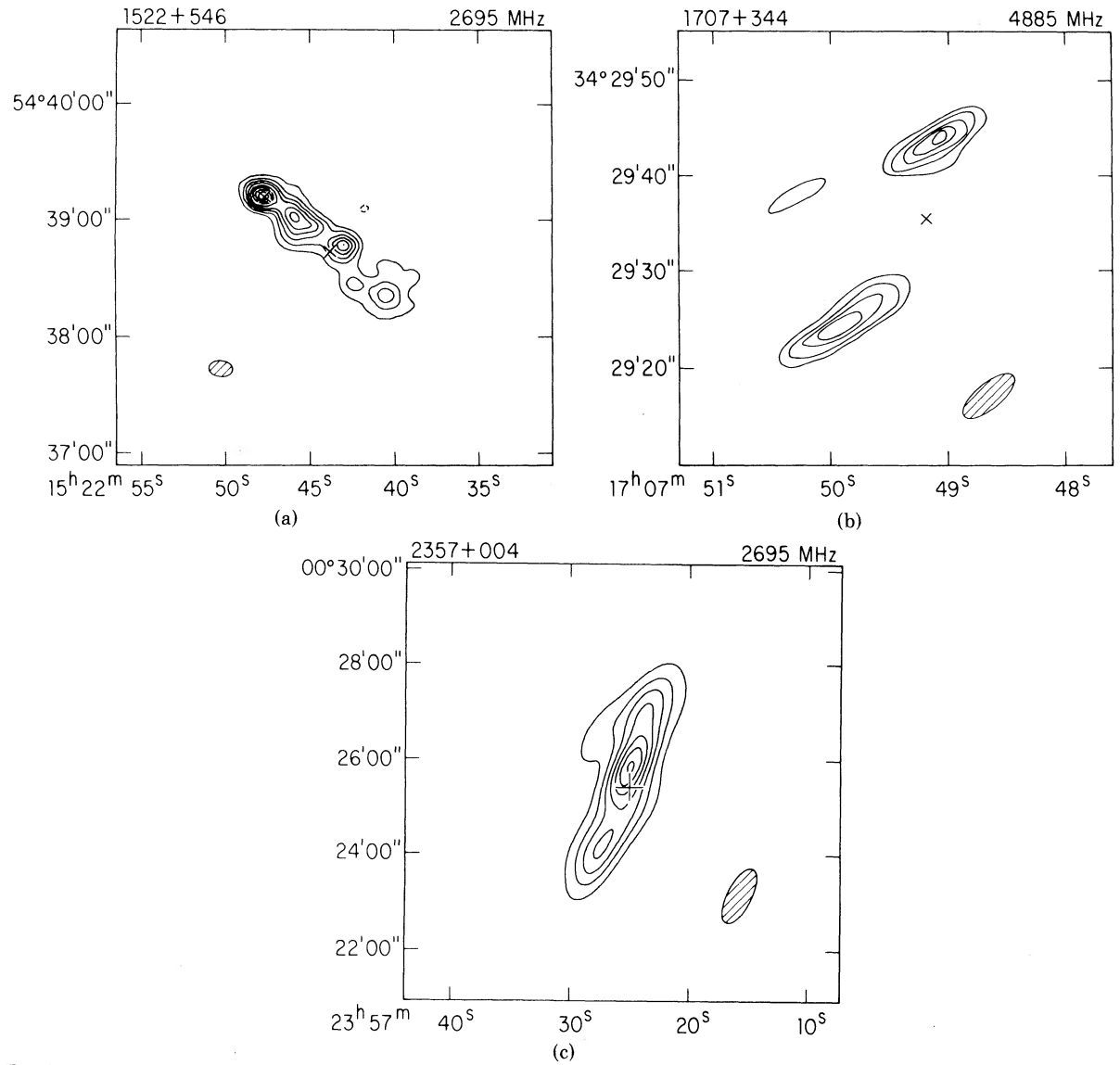

FIG. 2a. 1522 + 546: Each contour level is 31.1 mJy/beam. The location of a small-diameter component coincident with a 20^m optical object is shown by the *X* to the north. The identification suggested by Wyndham (1966), an $18.^m5$ galaxy, is shown by the *X* in the center.

FIG. 2b. 1707 + 344: Each contour level is 1.6 mJy/beam. The location of a 16^m galaxy is shown by the *X*. No small-diameter radio component was detected and several other galaxies lie between the components. See Rudnick and Owen (1977).

FIG. 2c. 2357 + 004: Each contour level is 12.6 mJy/beam. The location of a small-diameter component, coincident with a 16^m galaxy is shown by the +.

the VLA is located in the eastern galaxy. The nuclei are separated by 6 arcsec and are of equal brightness. A map of the extended structure is given in Paper I.

c) 0356 + 102 = 3C98

This component would be very close to the noise in the map at 5 GHz given by Jenkins *et al.* (1977), so our detection is consistent with their observation. The optical position has been measured by Griffin (1963).

d) 0915 + 320 = B2 0915 + 32

The large-scale structure of this source has been mapped in a full synthesis with six VLA antennas at 4.9 GHz by Fomalont and Bridle (1978), who also discuss the optical identification and its implications.

e) 1301 + 382 = 4C38.25

The 4.9-GHz map obtained at the VLA is shown in

© American Astronomical Society • Provided by the NASA Astrophysics Data System

1978AJ.....83..704B

Fig. 1c. The positions of two 19^m galaxies possibly associated with the source are also plotted. The source has a roughly double structure and there may be low-level emission from the vicinity of both galaxies. Further sensitive mapping will be needed to detect any radio core associated with this system and so resolve the identification ambiguity.

f) 1319 + 428 = 3C285

Jenkins *et al.* (1977) give an upper limit of 10 mJy for a small diameter, 5-GHz component anywhere in the source. This is consistent with our detection.

g) 1430 + 251 = 4C25.46

A map at 2.7 GHz made from NRAO interferometer data is shown in Fig. 1d. The small component detected at 4.9 GHz by the VLA is the northern component on this map. The only two optical objects in the radio field are shown and no radio emission >3 mJy was detected at 4.9 GHz from them. The nature and identification of this source or sources are unknown.

h) 1522 + 546 = 3C319

Our 2.7-GHz map obtained with the NRAO interferometer is shown in Fig. 2a. The optical identification has generally been taken to be the 18.^{m}5 galaxy (Wyndham 1966) near the center of this structure. No radio core is detected in the 18.^{m}5 galaxy [1950 position: 15^h 22^m 43.^{s}9 ± 0.^{s}1, 54° 38′ 42.″8 ± 1.″0 (Véron 1966)] to a limit of 4 mJy. The high-resolution map from the VLA shows, however, a small-diameter ($\lesssim$2″) component containing ~8% of the total emission at 4.9 GHz at the position marked in Fig. 2a. This feature has also been reported by Jenkins *et al.* (1977). The identification is complicated by the fact that this component coincides within the errors with a feature near the Sky Atlas print limit whose position measured on the Queen's University X–Y engine (Bridle and Goodson 1977) is 15^h 22^m 47.^{s}71 ± 0.^{s}05, +54° 39′ 10.″6 ± 0.″5,—epoch 1950. The optical positions of other objects in the field are given by Jenkins *et al.* (1977).

Three possible interpretations must be considered. First, the field may contain two unrelated radio systems, the VLA component being associated with the ~20^m object but the rest of 3C319 being associated with the 18.^{m}5 galaxy. Second, the field may be a single radio system associated with the 18.^{m}5 galaxy, as is now generally assumed. In this case the nature of the very faint optical object near the VLA component is of interest. Possibly it is a background object unrelated to the radio structure despite its proximity to the small component. The alternative exists, however, that the faint image is optical emission from a compact radio feature in 3C319, in which case observations of its optical spectrum and polarization are of considerable astrophysical importance. A third scenario would also consider the radio source to be a single physical system, the 20^m object being the optical identification of a head-tail structure. In this scenario the 18.^{m}5 galaxy would be assumed to be protected against the radio structure by chance. The 18.^{m}5 galaxy is in fact the brightest member of a fairly rich cluster in the field of the source, so this interpretation cannot be ruled out.

Final identification of this source must await more detailed radio mapping of the field and clarification of the nature of the faint image near the VLA radio component.

i) 2357 + 004

The VLA component lies in the western galaxy of a close pair proposed as the identification by Clarke *et al.* (1966). The galaxies are separated by 8 arcsec and the western galaxy is ~0.^{m}6 brighter on the O print of the Palomar Sky Atlas.

V. DISCUSSION

Except when the structural features of a source provide unambiguous morphological evidence for association with a galaxy (e.g., radio jets linking distant radio emission to a galaxy), identifications of extended sources are problematical. Two common criteria used to assist identifications—(a) small *a priori* probability of a particularly bright galaxy being situated within the radio emission and (b) small *a priori* probability of a galaxy positioned near the radio centroid or near a well-defined radio axis—may be insufficient to identify with confidence the galaxy associated with the radio emission. In many cases, however, detection of a radio core in an identification candidate can secure the identification of the extended source.

The utility of attempting to detect a small-diameter component which might indicate the location of the parent object (whether it is optically visible or not) depends on the *a priori* probability that the detected component lies within the extended area by chance. In Table IV we calculate for various source sizes the 5-GHz flux density at which there is less than 5% chance of random association. The source count used at 5 GHz (Fomalont *et al.* 1974) is

$$N = .027\, S^{-1.1},$$

where N is the number of sources per *square arc minute* with a flux density greater than S in *mJy units*. Although some of these weak sources will not be small in angular extent, we have shown in Paper I that some radio cores are extended so it may be appropriate to use the total source count to arrive at a conservative estimate of the probability of random coincidence. The "area covered by the source" was taken as the circular area whose angular diameter is the largest angular size (LAS). The "area near the centroid" was taken as a circular area

© American Astronomical Society • Provided by the NASA Astrophysics Data System

1978AJ.....83..704B

TABLE IV. Association of a radio core with an extended source with >95% confidence.

Largest angular size (arcsec)	Area covered by source (mJy)	Area near centroid (mJy)
300	>10.4	>1.2
60	>0.57	>0.06
15	>0.045	>0.005
3	>0.0024	>0.0003

centered on the source centroid with a radius of 0.15 LAS. In Paper I we showed that 90% of all bifurcated (double) sources are identified with galaxies in this latter area and this statistic can be used to limit the area of search for a radio core in a source whose detailed structure is adequately known.

Table IV demonstrates that if the angular extent exceeds several arcmin the detection of a random, small-diameter radio component within the source is not unlikely at the mJy flux density level. Confident identification of these extended sources will therefore require a combination of several of the morphological and brightness criteria used for the association of a radio source with an optical object unless the radio core is brighter than ~10 mJy. On the other hand, there will be very little likelihood of detecting *unrelated* small-diameter components within extended sources smaller than ~40 arcsec using the VLA in its completed state with a detection level of ~0.2 mJy at 1.4 and 5.0 GHz.

Eleven radio sources in the present sample of 21 contain a radio core brighter than 5 mJy at 4.9 GHz. The probability that the radio core lies in the area covered by each source is greater than one percent for 0136 + 397, 0356 + 102, 0915 + 320, 0936 + 361, 1319 + 428, 2058 − 135, and 2357 + 004 which has the largest probability of 5.3%. If we use the additional morphological criterion from Paper I that the identification of a bifurcated source normally lies within 15% of the largest angular size from the centroid (which is true for all of the above sources), the probability of misidentification is less than 0.5% in all cases. In addition, in all eleven sources, the optical object is the brightest galaxy in the structure, further supporting the identification according to the results of Paper I. The identification of two sources, 1430 + 251 and 1522 + 546, in which the small-diameter radio components are not near the centers of the structures, are unknown or ambiguous. The small components are associated with the extended source with ~99% confidence, however.

Of the eight sources in which no small-diameter component was detected, the identifications in the literature for 0802 + 243, 0819 + 061, 0938 + 399, 1308 + 277, and 1726 + 318 are probably reliable on the evidence of the brightness of the galaxies and their location near the centroids of the radio structures, although detection of a radio core would secure the identifications. The three sources 0258 + 356, 1301 + 382, and 1707 + 344 remain unidentified because there are several galaxies near the radio centroids.

We thank Mr. Greg Bothun for his help in the reductions, Dr. N. Vandenberg, Dr. R. Hjellming, and Dr. E. Greisen for their effort in the computing software, and the National Research Council of Canada for an operating grant to A.H.B. The National Radio Astronomy Observatory is operated by Associated Universities, Inc. under contract with the National Science Foundation.

REFERENCES

Branson, N. J. B. A., Elsmore, B., Pooley, G. G., and Ryle, M. (1972). Mon. Not. R. Astron. Soc. **156,** 377.

Bridle, A. H., Davis, M. M., Meloy, D. A., Fomalont, E. B., Strom, R. G., and Willis, A. G., (1976). Nature, **262,** 179.

Bridle, A. H., and Fomalont, E. B. (1978). Astron. J. **83,** 704.

Bridle, A. H., and Goodson, R. E. (1977). J. R. Astron. Soc. Can. **71,** 240.

Clarke, M. E., Bolton, J. G., and Shimmins, A. J. (1966). Aust. J. Phys. **19,** 375.

Colla, G., Fanti, C., Fanti, R., Gioia, I., Lari, C., Lequeux, J., Lucas, R., and Ulrich, M.-H., 1975, Astron. Astrophys. Suppl. **20,** 1.

Fomalont, E. B. (1971). Astron. J. **76,** 513.

Fomalont, E. B., and Bridle, A. H. (1978). Astrophys. J. Lett. In press.

Fomalont, E. B., Bridle, A. H., and Davis, M. M. (1974). Astron. Astrophys. **36,** 273.

Goodson, R. E., Palimaka, J. J., and Bridle, A. H. (1978) To be submitted to Astron. J. (Paper III).

Griffin, R. F. (1963). Astron. J. **68,** 421.

Högbom, J. A. (1974). Astron. Astrophys. Suppl. **15,** 417.

Högbom, J. A., and Carlsson, I. (1974). Astron. Astrophys. **34,** 341.

Jenkins, C. J., Pooley, G. G., and Riley, J. M. (1977). Mem. R. Astron. Soc. **84,** 61.

Maltby, P., Matthews, T. A., and Moffet, A. T. (1963) Astrophys. J. **137,** 153.

Merkelijn, J. K., Shimmins, A. J., and Bolton, J. G. (1968). Aust. J. Phys. **21,** 523.

Miley, G. K., and van der Laan, H. (1973). Astron. Astrophys. **28,** 359.

Olsen, E. T. (1970). Astron. J. **75,** 764.

Owen, F. N., Rudnick, L., and Peterson, B. M. (1977). Astron. J. **82,** 677.

Riley, J. J., and Pooley, G. G., (1975). Mon. Not. R. Astron. Soc. **80,** 105.

Rudnick, L., and Owen, F. N. (1977). Astron. J. **82,** 1.

Sargent, W. L. W. (1973). Astrophys. J. **182,** L13.

Schilizzi, R. T. (1975). Mem. R. Astron. Soc. **79,** 75.

Schilizzi, R. T., and McAdam, W. B. (1975). Mem. R. Astron. Soc. **79,** 1.

Véron, P. (1966). Astrophys. J. **144,** 861.

Willson, M. A. G. (1972). Mon. Not. R. Astron. Soc. **156,** 7.

Wyndham, J. D. (1966). Astrophys. J. **144,** 459.

© American Astronomical Society • Provided by the NASA Astrophysics Data System